Origin and evolution of the bread wheat D genome

https://doi.org/10.1038/s41586-024-07808-z

Received: 15 November 2023

Accepted: 10 July 2024

Published online: 14 August 2024

Open access

Check for updates

Emile Cavalet-Giorsa[1,42], Andrea González-Muñoz[1,42], Naveenkumar Athiyannan[1,42], Samuel Holden[2], Adil Salhi[3], Catherine Gardener[1], Jesús Quiroz-Chávez[4], Samira M. Rustamova[5], Ahmed Fawzy Elkot[6], Mehran Patpour[7], Awais Rasheed[8,9], Long Mao[10], Evans S. Lagudah[11], Sambasivam K. Periyannan[11,37], Amir Sharon[12], Axel Himmelbach[13], Jochen C. Reif[13], Manuela Knauft[13], Martin Mascher[13,14], Nils Stein[13,15], Noam Chayut[4], Sreya Ghosh[4], Dragan Perovic[16], Alexander Putra[17], Ana B. Perera[1], Chia-Yi Hu[1], Guotai Yu[1], Hanin Ibrahim Ahmed[1,38], Konstanze D. Laquai[1], Luis F. Rivera[1], Renjie Chen[1], Yajun Wang[1,39], Xin Gao[3], Sanzhen Liu[18], W. John Raupp[19], Eric L. Olson[20], Jong-Yeol Lee[21], Parveen Chhuneja[22], Satinder Kaur[22], Peng Zhang[23], Robert F. Park[23], Yi Ding[23], Deng-Cai Liu[24], Wanlong Li[25], Firuza Y. Nasyrova[26], Jan Dvorak[27], Mehrdad Abbasi[2], Meng Li[2], Naveen Kumar[2], Wilku B. Meyer[28], Willem H. P. Boshoff[28], Brian J. Steffenson[29], Oadi Matny[29], Parva K. Sharma[30], Vijay K. Tiwari[30], Surbhi Grewal[31], Curtis J. Pozniak[32], Harmeet Singh Chawla[32,40], Jennifer Ens[32], Luke T. Dunning[33], James A. Kolmer[34], Gerard R. Lazo[35], Steven S. Xu[35], Yong Q. Gu[35], Xianyang Xu[36], Cristobal Uauy[4], Michael Abrouk[1], Salim Bougouffa[3], Gurcharn S. Brar[2,41], Brande B. H. Wulff[1] ✉ & Simon G. Krattinger[1] ✉

Bread wheat (*Triticum aestivum*) is a globally dominant crop and major source of calories and proteins for the human diet. Compared with its wild ancestors, modern bread wheat shows lower genetic diversity, caused by polyploidisation, domestication and breeding bottlenecks[1,2]. Wild wheat relatives represent genetic reservoirs, and harbour diversity and beneficial alleles that have not been incorporated into bread wheat. Here we establish and analyse extensive genome resources for Tausch's goatgrass (*Aegilops tauschii*), the donor of the bread wheat D genome. Our analysis of 46 *Ae. tauschii* genomes enabled us to clone a disease resistance gene and perform haplotype analysis across a complex disease resistance locus, allowing us to discern alleles from paralogous gene copies. We also reveal the complex genetic composition and history of the bread wheat D genome, which involves contributions from genetically and geographically discrete *Ae. tauschii* subpopulations. Together, our results reveal the complex history of the bread wheat D genome and demonstrate the potential of wild relatives in crop improvement.

Bread wheat (*T. aestivum*) is one of the most widely cultivated and most successful crop species worldwide, and has a pivotal role in the global food system. Modern bread wheat shows a remarkably wide geographical distribution and adaptability to various climatic conditions[1]. Current yield gains, however, might be insufficient to meet future bread wheat demands[3], which calls for concerted efforts to diversify and intensify wheat breeding to further raise yields. Bread wheat is an allohexaploid species ($2n = 6x = 42$, AABBDD genome) whose evolution involved the hybridization of three wild grass species. An initial hybridization between the A genome donor *Triticum urartu* ($2n = 2x = 14$) and an unknown B genome donor related to the goatgrass *Aegilops speltoides* gave rise to tetraploid wild emmer wheat (*Triticum turgidum* subsp. *dicoccoides*, $2n = 4x = 28$, AABB genome) 0.5–0.8 million years ago[4]. The second hybridization event happened between a domesticated tetraploid wheat and the D genome progenitor Tausch's goatgrass (*Ae. tauschii*; $2n = 2x = 14$, DD genome). This hybridization that gave rise to bread wheat most probably occurred along the southern shores of the Caspian Sea 8,000–11,000 years ago[5,6]. Polyploidization and domestication events such as the origin of bread wheat represent extreme genetic bottlenecks[1,2,7,8]. In the case of bread wheat, recurrent hybridizations with wild wheat relatives and other domesticated wheat species have significantly increased genetic diversity following domestication[2,9–13]. The underlying gene flow contributed to the adaptability of bread wheat to diverse climatic conditions outside the Fertile Crescent, the geographical region where wheat was domesticated. Compared with the A and B genomes, however, D genome diversity in bread wheat remains low because the above gene flow has predominantly involved tetraploid species with an AB genome[2,6,10,14].

Here we establish a comprehensive set of genomic resources for the bread wheat D genome progenitor *Ae. tauschii*, including whole-genome sequencing (WGS) data of a large *Ae. tauschii* diversity panel and chromosome-scale assemblies representing the three *Ae. tauschii* lineages. The genomic resources proved useful for haplotype and gene discovery and enabled us to unravel the composition and evolution of the bread wheat D genome.

A list of affiliations appears at the end of the paper.

Genomic resources for *Ae. tauschii*

To comprehensively assess genetic diversity in *Ae. tauschii*, we first compiled a presence–absence *k*-mer matrix from a diversity panel comprising 920 sequenced *Ae. tauschii* accessions (Supplementary Table 1 and Supplementary Note 1). We optimized the *k*-mer matrix workflow for large diversity panels (Supplementary Note 2) using WGS data from this and previous studies[14,15] (Supplementary Table 1). The *k*-mer analysis revealed 493 non-redundant *Ae. tauschii* accessions, whereas the remaining accessions shared at least 96% of their *k*-mers with a given non-redundant accession (Supplementary Table 2). The non-redundant diversity panel spanned the geographical range of *Ae. tauschii* from northwestern Turkey to eastern China (Fig. 1a) and defined a phylogeny demarcated by the 3 basal lineages, with 335 accessions for lineage 1 (L1), 150 accessions for lineage 2 (L2) and 8 accessions for lineage 3 (L3) (Fig. 1b).

We performed single nucleotide polymorphism (SNP)-based phylogenetic (Fig. 1b and Extended Data Fig. 1a) and ancestry analyses (Extended Data Fig. 2) on the diversity panel, which defined four geographically distinct subpopulations for *Ae. tauschii* L2, referred to as L2E-1 (southwestern Caspian Sea), L2E-2 (southeastern Caspian Sea), L2W-1 (Caucasus) and L2W-2 (Turkmenistan and northern Iran), in accordance with the literature[5,15]. Group L2E from the southern Caspian Sea (representing subpopulations L2E-1 and L2E-2 here) was previously identified as the main contributor of the bread wheat D genome[5]. Of the 150 non-redundant *Ae. tauschii* L2 accessions, we could assign 133 to one of the four L2 subpopulations on the basis of an ancestry threshold of greater than or equal to 70% (Supplementary Table 3). The remaining 17 L2 accessions were considered admixed.

Using genetic, geographical and phenotypic diversity, we selected 46 accessions to construct high-quality genome assemblies, comprising 11 L1 accessions, 34 L2 accessions and 1 L3 accession (Fig. 1a,b and Supplementary Table 4). The 46 accessions captured 72.5% of the genetic diversity present in the *Ae. tauschii* diversity panel based on *k*-mer analysis. The majority of the *k*-mers that were not captured in the 46 high-quality assemblies are rare and were found in fewer than 5% of the accessions that make up the *Ae. tauschii* diversity panel (Extended Data Fig. 1b,c and Supplementary Table 5). We sequenced the selected 46 accessions by PacBio circular consensus sequencing[16] to a median genome coverage of 23-fold (18- to 47-fold) and generated primary contig-level assemblies with contig N50 values ranging from 15.02 Mb to 263.79 Mb (median 45.26 Mb) (Supplementary Table 6). Phred quality scores ranged from 34.9 to 48.3 (median 45.5) and *k*-mer completeness scores ranged from 95.1 to 99.8% (median 99.4%) based on 21-mer content comparison with short-read WGS data (Supplementary Table 6). We calculated the benchmarking universal single-copy orthologues (BUSCO) scores for each accession[17], returning values between 98.0% and 98.6% (Supplementary Table 6), indicating high contiguity, accuracy and completeness of the assemblies. We selected one representative accession per lineage to generate de novo annotated pseudochromosome assemblies, namely TA10171 (L1), TA1675 (L2) and TA2576 (L3). For these three accessions, we increased the sequencing coverage to 67- to 97-fold, generated assemblies with contig N50 values of 53.38 Mb (L1), 221.04 Mb (L2) and 116.91 Mb (L3) (Supplementary Table 6), and used Hi-C chromatin conformation capture[18] to scaffold the assemblies into pseudomolecules (Extended Data Table 1 and Extended Data Fig. 3a–c). De novo annotation of the three chromosome-scale assemblies revealed 43,511 to 44,275 protein-coding genes (Extended Data Table 1). We included five previously generated high-quality *Ae. tauschii* assemblies[15,19] and the bread wheat D genome[20] for a gene cluster analysis. In total, we identified 52,722 clusters, of which 18,835 and 33,953 were core and dispensable, respectively (Supplementary Table 7). We then scaffolded the remaining 43 L1 and L2 contig-level assemblies using their respective L1 and L2 chromosome-scale references as guides (Supplementary Table 6).

In accordance with previous observations[5,14,21], we detected increased nucleotide diversity in L2 ($\pi = 0.00038$) compared with L1 and L3 (L1, $\pi = 0.00021$; L3, $\pi = 0.00024$) (Fig. 1c and Supplementary Table 8). Structural variants were called across the high-quality assemblies relative to the TA1675 (L2) reference assembly (Fig. 1c). L1 accessions showed a similar distribution of structural variants to that in the L3 accession TA2576 (Extended Data Fig. 1d), with a median of 205,856 and 191,179 structural variants per accession for L1 and L3, respectively (Supplementary Table 9). The L2 accessions had a median of 85,401 structural variants per accession compared with the TA1675 reference (Supplementary Table 9).

Gene discovery

The highly contiguous *Ae. tauschii* assemblies generated here present an opportunity for gene discovery and characterization by comparative haplotype analyses. Here, we assessed the value of the *Ae. tauschii* genomic resources with a focus on rust resistance genes. The three fungal wheat rust diseases, leaf rust (caused by *Puccinia triticina* (*Pt*)), stripe rust (*P. striiformis* f. sp. *tritici*) and stem rust (*P. graminis* f. sp. *tritici* (*Pgt*)), are among the most devastating and most ubiquitous wheat diseases, causing considerable yield losses[22]. The stem rust resistance gene *SrTA1662* was introgressed into bread wheat from *Ae. tauschii* accession TA1662 and genetically mapped to the stem rust resistance locus *SR33* on chromosome arm 1DS[23,24]. Because the original mapping could not establish whether the stem rust resistance gene from TA1662 was a new gene or was allelic to *Sr33*, the gene was given the temporary designation *SrTA1662*[23]. *Sr33* and *SrTA1662* encode intracellular nucleotide-binding leucine-rich repeat (NLR) immune receptors belonging to the *Mla* family[14,24,25]. Here, we repeated the *k*-mer-based association mapping that led to the initial discovery of the *SrTA1662* candidate gene[14]. Compared with the short-read based *Ae. tauschii* assemblies[14], mapping the *k*-mers against our high-quality *Ae. tauschii* genome strongly decreased the noise in the *k*-mer-based association approach (Fig. 2a). A detailed haplotype analysis revealed that *SrTA1662* is a paralogue rather than an allele of *Sr33* (Fig. 2b, Extended Data Fig. 4a and Supplementary Table 10). When we compared the stem rust infection phenotypes of *Ae. tauschii* lines predicted to carry only *Sr33* or *SrTA1662*, we observed that the two genes appeared to have different specificities (Supplementary Table 11). We confirmed this notion by inoculating *SrTA1662* transgenic wheat lines[14] and *Sr33* introgression lines with five *Pgt* isolates (Extended Data Fig. 4b and Supplementary Table 12). Our analysis so far showed that *SrTA1662* confers resistance to a subset of the *Pgt* isolates avirulent on *Sr33*. In line with the nomenclature standards for wheat gene designation[26], we therefore renamed *SrTA1662* to *Sr66*.

Ae. tauschii accession TA1675, for which a chromosome-scale reference assembly was generated in this study, carries the leaf rust resistance gene *Lr39*, which was mapped to the short arm of chromosome 2D[27,28]. *k*-mer-based association mapping with the *Pt* isolate BBBDB (avirulent against *Lr39*)[29] revealed a peak at the telomeric end of chromosome arm 2DS, corresponding to the 2.33–2.45 Mb region in the TA1675 assembly (Fig. 2c). This location overlapped with markers flanking *LR39* (positions 1.20–2.84 Mb) that were identified based on bi-parental genetic mapping[30] (Fig. 2c and Extended Data Fig. 5a,b). The genomic region underlying the association peak contained 3 candidate genes in TA1675 (1 wheat tandem kinase (WTK) and 2 genes of unknown function), and the interval identified through bi-parental mapping harboured 16 genes (Supplementary Table 13). On the basis of functional annotations and polymorphisms compared with the susceptible *Ae. tauschii* accession AL8/78, the most promising candidate was *AeT.TA1675.r1.2D000150*, which encodes a WTK, a protein family that has a prominent role in disease resistance in wheat[31–33]. Virus-induced gene silencing (VIGS) of the WTK candidate gene in TA1675 resulted in greater susceptibility to leaf rust (Fig. 2d and Extended Data Fig. 5c).

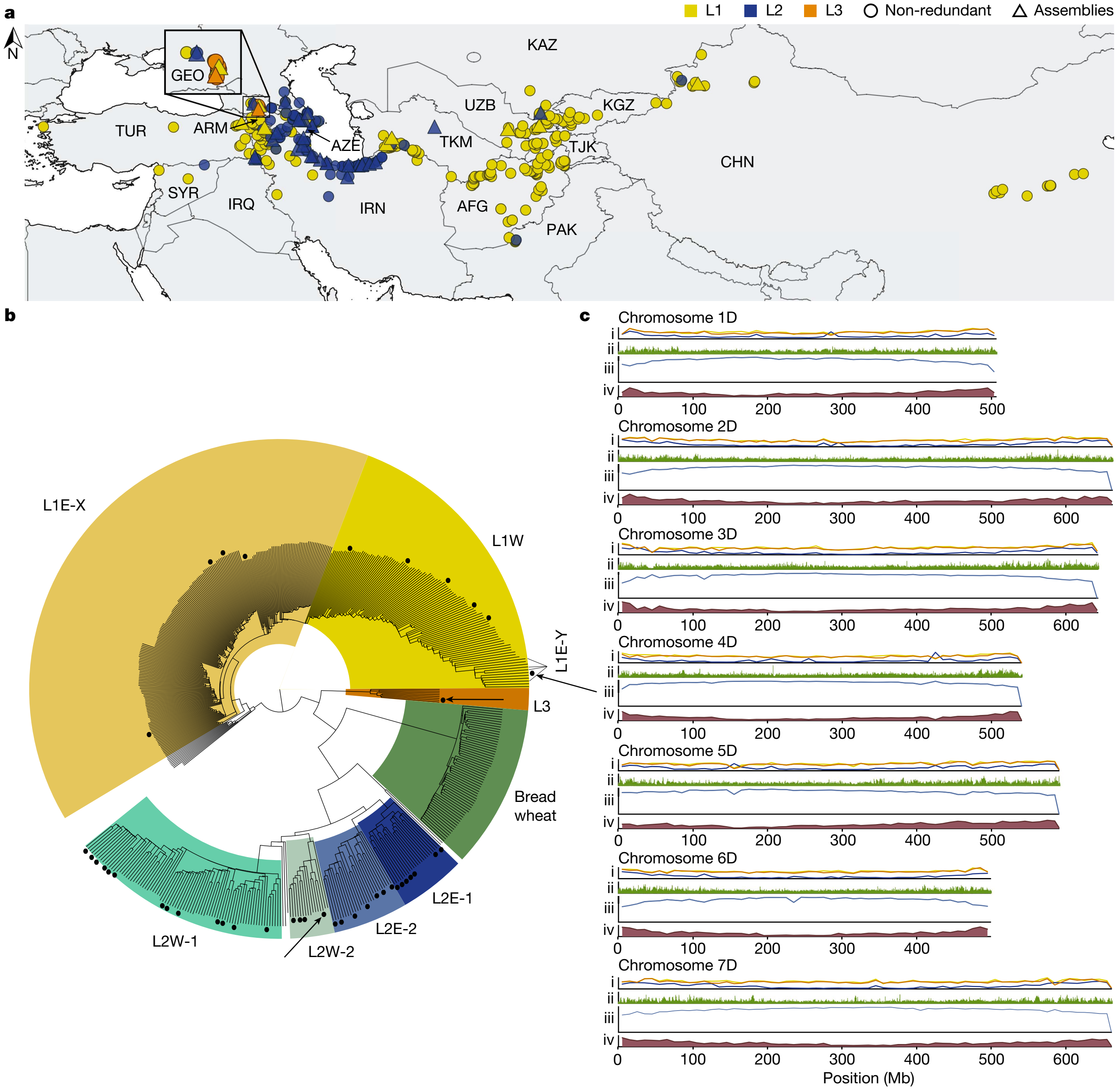

Fig. 1 | The *Ae. tauschii* diversity panel and genomes. a, Geographical distribution of the 493 non-redundant *Ae. tauschii* accessions in the diversity panel. Accessions selected to generate high-quality assemblies are indicated by triangles coloured according to their respective lineage. AFG, Afghanistan; ARM, Armenia; AZE, Azerbaijan; CHN, China; GEO, Georgia; IRQ, Iraq; IRN, Islamic Republic of Iran; KAZ, Kazakhstan; KGZ, Kyrgyzstan; PAK, Pakistan; SYR, Syrian Arab Republic; TJK, Tajikistan; TKM, Turkmenistan; TUR, Türkiye; UZB, Uzbekistan. **b**, SNP-based phylogeny of the non-redundant *Ae. tauschii* accessions showing the subpopulations within the three lineages as labelled on the tree. Accessions sequenced with PacBio HiFi are indicated by black dots next to the tree branches. The three reference accessions TA10171 (L1), TA1675 (L2) and TA2576 (L3) are indicated by black arrows. The D subgenome from 59 wheat landraces is shown in relation to *Ae. tauschii*. **c**, Linear chromosome representation showing structural variants, nucleotide diversity and annotation features across the *Ae. tauschii* panel and genomes relative to the TA1675 L2 reference assembly. The tracks show (i) mean structural variant density in 10 Mb windows for L1 (yellow), L2 (blue) and L3 (orange) accessions of the 46 high-quality assemblies (range 0–800 structural variants), (ii) nucleotide diversity in 10-kb windows across the diversity panel of 493 non-redundant *Ae. tauschii* accessions (π = 0–0.0045), (iii) repeat density in TA1675 in 10-Mb windows (range 1–10 million repeat-masked nucleotides), and (iv) gene density in TA1675 in 10-Mb windows (range 0–350 high-confidence genes).

Silencing of an NLR-encoding gene (*AeT.TA1675.r1.2D000200*) located just outside the peak region did not result in increased susceptibility (Fig. 2c,d), indicating that the WTK gene is *Lr39*. The predicted genomic sequence of the *Lr39* candidate gene is 11,699 bp in length with 21 exons. The corresponding 3,408-bp coding sequence encodes an 1,135-amino acid protein with two N-terminal kinase domains of the LRR_8B subfamily, followed by a major sperm protein domain and a WD40 repeat-containing domain (WD40) at the C terminus (Fig. 2e and Extended Data Fig. 5d). Compared with the susceptible *Ae. tauschii* accession AL8/78, Lr39 from TA1675 carried two amino acid changes located in the kinase 2 and WD40 domains, respectively (Fig. 2e and Extended Data Fig. 5d).

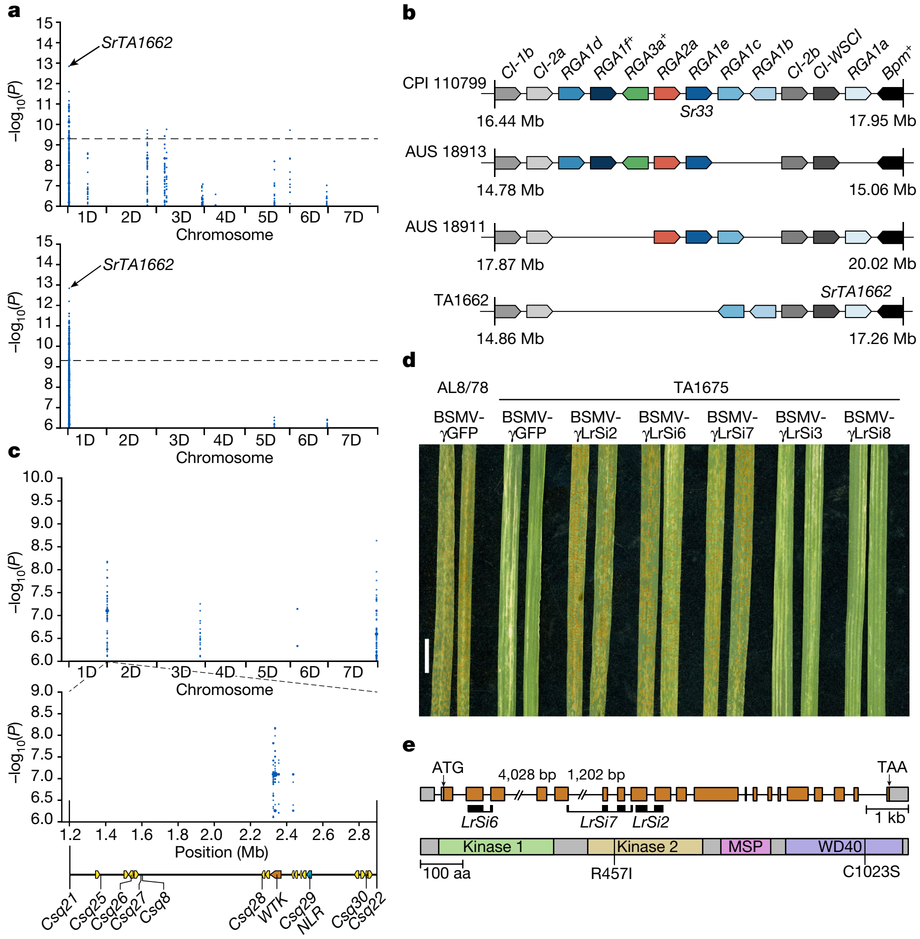

Fig. 2 | Haplotype analyses and cloning of a disease resistance gene. a, Effect of assembly quality on association genetics. Significantly associated *k*-mers for resistance to *Pgt* race QTHJC mapped to two *Ae. tauschii* TA1662 assemblies (top, low-quality, contig N50 = 196 kb (ref. 14); bottom, high-quality, contig N50 = 58.21 Mb (this study)). The chromosome arm 1DS disequilibrium block contains the stem rust resistance gene *SrTA1662* (renamed *Sr66*). **b**, Different *Mla* haplotypes[24] reflected by analysis of resistance gene analogues (RGA) in *Ae. tauschii* CPI 110799 (*Sr33* donor), AUS 18913, AUS 18911 and TA1662 (*SrTA1662* donor). Boxes indicates genes; + indicates pseudogenes. Alleles are indicated by matching colour and position. The locus is flanked by subtilisin-chymotrypsin inhibitor (*CI*, grey) and pumilio (*Bpm*, black) genes. Unrelated genes present in this region are omitted. Locus length and gene distribution are not drawn to scale. **c**, *k*-mer-based genome-wide association study (GWAS) with *Pt* race BBBDB mapped to the *Ae. tauschii* TA1675 assembly. The chromosome arm 2D peak corresponds to leaf rust resistance locus *LR39*. The diagram shows the *LR39* interval delimited by bi-parental mapping, flanked by markers *Csq21* and *Csq22*, and markers *Csq8* and *Csq25*-*Csq30* co-segregating with *LR39*. Arrows indicate candidate genes. **d**, Effects of VIGS on susceptibility to leaf rust. AL8/78, susceptible control; BSMV-γGFP, barley stripe mosaic virus (BSMV) expressing a GFP silencing construct (control); BSMV-γLrSi2, BSMV-γLrSi6 and BSMV-γLrSi7 are silencing constructs specific for the WTK gene. BSMV-γLrSi3 and BSMV-γLrSi8 are silencing construct specific for the *NLR* gene. Probe specificities were evaluated using the TA1675 assembly. Chlorosis in BSMV-γGFP controls represent virus symptoms. Scale bar, 1 cm. **e**, Gene structure of *Lr39* (top) and domain architecture of the Lr39 protein (bottom). Grey boxes represent untranslated regions, orange boxes are exons and lines are introns. VIGS probes are indicated. R457I and C1023S indicate the two Lr39 amino acid changes between the TA1675 (resistant) and AL8/78 (susceptible) lines. MSP, major sperm protein domain.

Several recent studies have highlighted the importance of using genome assemblies of resistance gene-containing reference accessions for gene cloning and designation[11,34]. The analyses we present here would have been difficult, if not impossible, using previous *Ae. tauschii* assemblies, because none of them are donors of *Sr33*, *SrTA1662* (*Sr66*) or *Lr39*.

Lineage-specific haplotype blocks

Bread wheat has become one of the most successful and widely cultivated crop species, and is adapted to a wide range of climatic conditions[1]. Continuous gene flow by natural and artificial introgressions from wild wheat relatives has increased the genetic diversity of bread wheat following a domestication bottleneck[9–13]. For example, around 1% of the extant bread wheat D genome originated from *Ae. tauschii* L3, indicating multiple hybridization events that gave rise to the extant bread wheat D genome[14]. The genetic distinctness and geographical restriction of *Ae. tauschii* L3 (Fig. 1a,b) makes this lineage an ideal example to study the spatial dynamics of introgressions. We hypothesize that bread wheat landraces with higher L3 genome content, possibly representing a more ancestral state of the L3 introgression(s), have been preserved in ex situ collections but are rare and geographically restricted.

To identify bread wheat accessions with above-average proportions of L3 genome, we developed the 'Missing Link Finder' pipeline (Fig. 3a). Missing Link Finder estimates the similarity between a species- or lineage-specific reference *k*-mer set and sample *k*-mer sets generated from genotyping data of individual wheat accessions, computing the result as Jaccard similarity coefficients. To deploy Missing Link Finder, we used a reference *k*-mer set consisting of 769 million *Ae. tauschii* L3-specific *k*-mers[14] and compared it to individual sample *k*-mer sets from 82,293 genotyped wheat accessions (6.16 million *k*-mers per

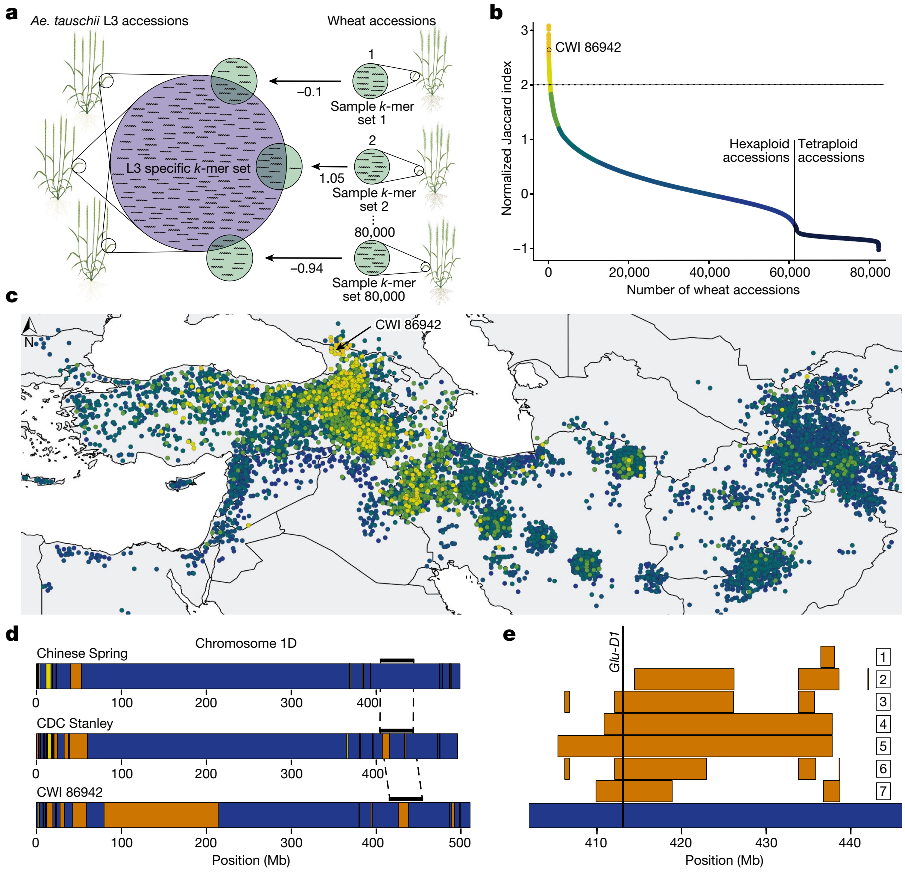

Fig. 3 | *Ae. tauschii* L3 introgressions in bread wheat. a, Diagram of the Missing Link Finder pipeline. An *Ae. tauschii* L3-specific *k*-mer set (769 million L3-specific *k*-mers; blue circle) was compared to individual sample *k*-mer sets generated from more than 80,000 genotyped wheat accessions (green circles). The result is indicated as normalized Jaccard indices. **b**, Distribution of normalized Jaccard scores across 82,154 wheat accessions. The horizontal dotted line indicates the two-fold threshold. The 139 synthetic hexaploid wheat lines with increased Jaccard indices have been removed and are shown in Extended Data Fig. 6a. **c**, The Jaccard indices show a gradual decline with increasing geographical distance from Georgia. Dots represent individual bread wheat accessions for which exact coordinates were available. Colours represent different normalized Jaccard indices corresponding to **b**. A full map is shown in Extended Data Fig. 6b. Eastern bread wheat accessions from Tajikistan with high Jaccard indices carry the same L3 introgression segments as bread wheat landraces from Georgia, indicating a common origin of the L3 haplotype blocks (Supplementary Table 18). **d**, Diagram of chromosome 1D in the wheat lines Chinese Spring, CDC Stanley and CWI 86942. Haplotype blocks corresponding to *Ae. tauschii* L1 are indicated in yellow, L2 is indicated in blue, and L3 is in orange. The black bars above the chromosome indicate the region shown in **e**. **e**, Diagram of a portion of the long arm of bread wheat chromosome 1D. Shown are different lengths of the L3 introgression segment in various bread wheat lines. The numbers correspond to the following accessions chosen for their diverse recombination patterns in this locus: (1) CWI 86929; (2) CWI 30140; (3) CWI 57175; (4) CWI 84686; (5) CWI 84704; (6) CWI 86481; (7) CDC Stanley.

accession on average)[35]. We identified 503 bread wheat accessions with an above-average (more than twofold) normalized Jaccard index (a value of 0 indicates an average number of L3 *k*-mers), indicative of increased *Ae. tauschii* L3 content (Fig. 3b and Extended Data Fig. 6a). The 139 accessions with the highest Jaccard indices are synthetic hexaploid wheats (Extended Data Fig. 6a), most of which (122 accessions) were produced using an *Ae. tauschii* accession collected in Georgia (CWI 94855), the only country where *Ae. tauschii* L3 has been found in the present day[14]. We also identified 364 bread wheat landraces with putatively increased proportions of L3 introgressions (Fig. 3b and Extended Data Fig. 6a). One of the bread wheat landraces with the highest Jaccard indices, CWI 86942 (PI 572674), was collected in the Samegrelo-Zemo Svaneti region of Georgia[36]. We observed a gradient of decreasing L3 proportions (as revealed by Jaccard indices) with increasing geographical distance from Georgia (Fig. 3c and Extended Data Fig. 6b).

To further quantify and explore the L3 contents of CWI 86942 and other landraces, we generated an annotated chromosome-scale assembly of CWI 86942 using PacBio circular consensus sequencing[16] and chromosome conformation capture[18] (Extended Data Table 1 and Extended Data Fig. 3d). In addition, we produced WGS data (tenfold coverage) of 36 hexaploid wheat landraces with higher (greater than 2) Jaccard indices using short-read Illumina-based sequencing. For comparison, we also sequenced 23 wheat landraces with Jaccard indices of less than 2 (Supplementary Table 14). Our analysis focused on landraces to avoid detection of L3 haplotype blocks that might be the result of artificial introgressions. We observed a good correlation between the Jaccard indices and the *Ae. tauschii* L3 content estimated based on WGS data (Extended Data Fig. 6c), supporting the idea that Missing Link Finder is a suitable pipeline to identify rare wheat accessions with above-average introgressions. CWI 86942 contained approximately 7.0% of L3 introgressions, compared with the 0.5 to 1.9% in other bread wheat assemblies[14]. Most notable was a 135-Mb L3 segment in the pericentromeric region of chromosome 1D (Fig. 3d), which represents the largest *Ae. tauschii* L3 haplotype block reported in bread wheat so far. This segment contains 587 predicted genes, of which 112 showed presence–absence variation or a disruptive mutation compared to the corresponding L2 segment in wheat cultivar Kariega (Supplementary Table 15). In addition to CWI 86942, this L3 haplotype segment, or parts thereof, were found in multiple bread wheat landraces collected between the 1920s and the 1930s (Extended Data Fig. 6d),

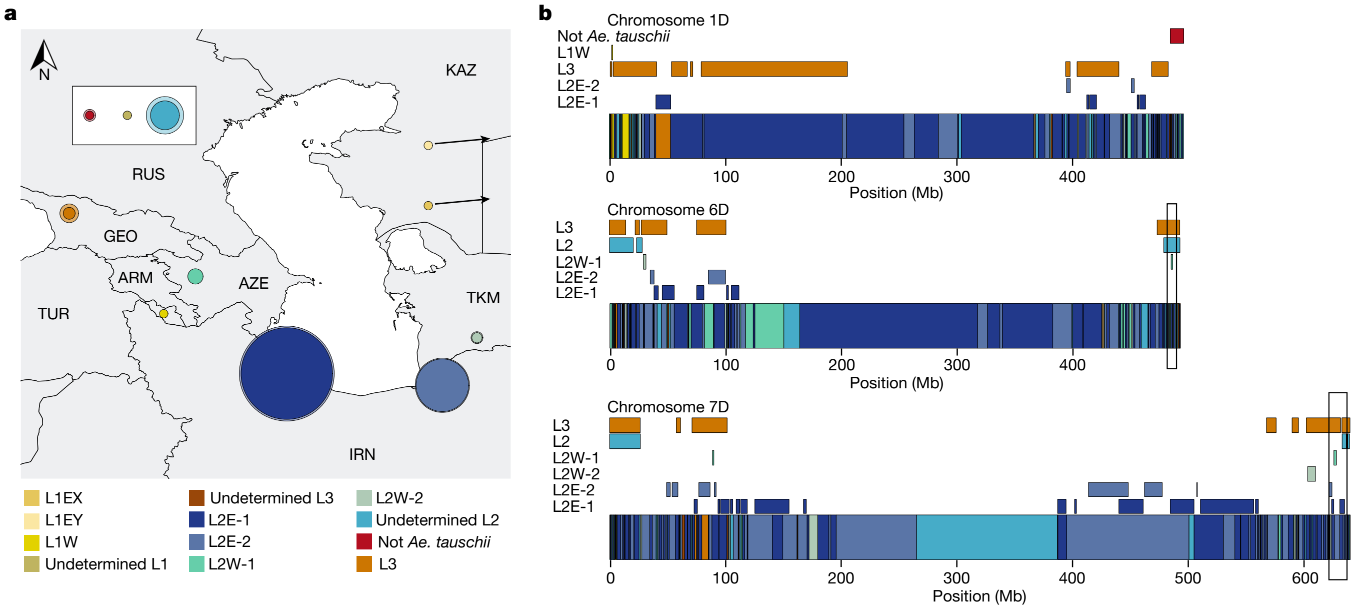

Fig. 4 | Different *Ae. tauschii* subpopulations contributed to the hexaploid wheat D genome. a, Proportions of *Ae. tauschii* subpopulations that make up the wheat D genome. Inner circles in solid colours represent the average proportions across 17 hexaploid wheat assemblies. The outer lighter circles represent the maximum proportion found across the 17 wheat genomes. The geographical location for each subpopulation was assigned on the basis of representative accessions. RUS, Russian Federation. **b**, Minimal number of hybridization events that gave rise to the extant bread wheat D genome. Diagrams show chromosomes 1D, 6D and 7D in Chinese Spring. The coloured boxes along the chromosomes represent the haplotypes present in Chinese Spring. Coloured rectangles above the chromosomes represent alternative haplotype blocks identified across 126 hexaploid wheat landraces (cumulative length of alternative haplotype blocks across all 126 landraces). Colours refer to the *Ae. tauschii* subpopulations. The maximum number of haplotype blocks was four. Black boxes highlight the regions on chromosome 3D and 7D in which four overlapping haplotypes are found.

indicating that this segment is not the result of synthetic hexaploid wheat breeding[37,38]. A second notable L3 segment was found on the long arm of chromosome 1D in multiple bread wheat landraces (Fig. 3e). This segment carries a superior wheat quality allele at the *Glu-D1* locus that originated from *Ae. tauschii* L3[39]. In modern bread wheat (for example, wheat cultivars CDC Landmark, CDC Stanley and Jagger), this L3 segment is around 8.5 Mb in size. We identified a group of bread wheat landraces originating from Azerbaijan where the corresponding L3 segment was up to 36.35 Mb in size (Fig. 3e). This L3 introgression showed various lengths in different bread wheat landraces, reflecting extensive recombination. We further estimated the cumulative proportion of L3 introgression across a comprehensive set of 126 hexaploid wheat landraces, including the WGS data from the 59 landraces generated in this study and publicly available sequencing data (Supplementary Table 16). Using identity-by-state, we determined that 16.6% of the wheat D genome, corresponding to 666.0 Mb and containing 8,779 high-confidence genes (25.6%), can be covered with *Ae. tauschii* L3 haplotype blocks across these landraces (Supplementary Table 17). Although the proportion of *Ae. tauschii* L3 introgressions in most modern bread wheat cultivars is marginal (approximately 1% relative to the entire D genome), the cumulative size of L3 introgressions across multiple bread wheat landraces is considerable.

Origin and evolution of the wheat D genome

We determined the complexity and origin of the D genome across 17 hexaploid wheat lines, for which chromosome-scale assemblies are available[11,34,40,41,20,42,43]. We divided the wheat genomes into 50-kb windows and assigned each window to an *Ae. tauschii* subpopulation based on identity-by-state[13]. We observed that all four *Ae. tauschii* L2 subpopulations contributed genomic segments to the bread wheat D genome (Supplementary Table 19). Consistent with previous reports[5], the largest proportion of the wheat D genome (45.6–51.3%) originated from subpopulation L2E-1, which is mainly found in the southwestern Caspian Sea region. Subpopulation L2E-2 (southeastern Caspian Sea) contributed 24.7–27.3% to the wheat D genome (Fig. 4a). Up to 6.9% of the wheat D genome was identical (based on identity-by-state analysis) to *Ae. tauschii* subpopulation L2W, with 4.1-5.0% coming from subpopulation L2W-1 and subpopulation L2W-2 contributing 1.7–2.2% (Fig. 4a,b and Extended Data Fig. 7). We could assign another 10.7–19.5% of the wheat D genome to L2, but without being able to infer the exact subpopulation (Supplementary Note 3), indicating that these segments originated from *Ae. tauschii* L2 haplotypes that were not captured in our diversity panel (Fig. 4a,b and Extended Data Fig. 7). The contributions from *Ae. tauschii* L1 and L3 ranged from 0.7% to 1.1% and 1.6% to 7.0%, respectively. Genomic windows representing 0.1–2.4% of the hexaploid wheat D genome had a different origin than *Ae. tauschii*. These windows include previously described introgressions, such as the tall wheatgrass (*Thinopyrum ponticum*) introgression on chromosome 3D in bread wheat cultivar LongReach Lancer or the putative *Aegilops markgrafii/Aegilops umbellulata* introgression on chromosome 2D of cultivars Julius, Arina*LrFor*, SY Mattis and Jagger[11,12] (Supplementary Table 19). A list of predicted genes and their corresponding subpopulation origin is provided in Supplementary Table 20. The number of *Ae. tauschii* subpopulations that contributed to the hexaploid wheat D genome does not necessarily reflect the number of independent hybridization events, because the *Ae. tauschii* line that contributed the D genome may have already been admixed. To infer the minimal number of hybridizations that gave rise to the extant wheat D genome, we assessed the number of haplotypes present at any given position in the wheat D genome. We used Chinese Spring as a reference and identified 50-kb windows showing no identity-by-state across the 126 hexaploid wheat landraces for which WGS data were available. Such windows indicate the presence of at least two haplotypes in the hexaploid wheat gene pool. Consecutive 50-kb windows with no identity-by-state were concatenated into alternative haplotype blocks. The origins of alternative haplotype blocks were then assigned to one of the *Ae. tauschii* subpopulations using identity-by-state (Supplementary Table 21). In total, 71.4% of the wheat D genome was covered by a single haplotype across the analysed hexaploid wheat lines (59.7% of genes). The remaining 28.6% of the wheat D genome showed multiple haplotypes (21.0% of the wheat D genome had two haplotypes (26.2% of genes), 6.7% had three haplotypes (12.2% of genes) and 0.9% had four haplotypes (1.9% of genes)) (Fig. 4b, Extended Data Fig. 7 and Supplementary Table 22). The maximum number of haplotypes corresponding to different *Ae. tauschii* subpopulations for any given window was four, indicating that the bread wheat D genome evolved through at least four hybridizations.

Discussion

The comprehensive genomic resources generated in this study enabled haplotype analysis and cloning of rust resistance genes and they offered a detailed insight into the composition and origin of the bread wheat D genome. Crop domestication has often been considered as a relatively simple linear progression[44]. Our analyses support a model of protracted domestication that is more complex, involving recurring episodes of hybridization and gene flow that resulted in patchwork-like haplotype patterns across the bread wheat D genome. We largely confirm that an *Ae. tauschii* L2 population from the southwestern Caspian Sea region was the major donor of the bread wheat D genome[5] (Fig. 4a), with smaller genomic segments originating from different *Ae. tauschii* lineages[5,14]. In contrast to previous reports, however, our work revealed a much more complex patterning of the bread wheat D genome. We determined that all four L2 subpopulations, as well as L1 and L3, contributed segments to the extant bread wheat D genome. Compared to the AB subgenomes, the bread wheat D genome shows a lower genetic diversity, indicative of a much lower rate of introgression from wild progenitors[2,6]. The patchwork pattern seen in the bread wheat D genome is somewhat surprising given that most *Ae. tauschii* L2 accessions in our diversity panel showed a low degree of admixture, with a well-defined population structure following their geographical distribution (Extended Data Fig. 2). A possible explanation for this observation is that the *Ae. tauschii* accession that gave rise to the bread wheat D genome was admixed, carrying genomic segments from different subpopulations. Remnants of *Aegilops* species have been identified at several pre-agricultural settlements in the Fertile Crescent[45], indicating that *Aegilops* species were used as food source or persisted as weeds in pre-agricultural cultivation of other wild cereals. The gathering and possible management of *Ae. tauschii* for food, or its co-cultivation as a weed over an extended period might have resulted in mixing of *Ae. tauschii* populations with different geographical origins, leading to an increase of admixed accessions close to human settlements. Such an admixed *Ae. tauschii* population might have later given rise to the bread wheat D genome. This scenario would also explain why the bread wheat D genome forms a separate clade from *Ae. tauschii* in many phylogenetic and population structure analyses[5,14,15,46] (Fig. 1b). Alternatively, the *Ae. tauschii* accession that gave rise to the bread wheat D genome was non-admixed, and recurrent hybridizations resulted in the observed mosaic-like haplotype pattern.

Another important finding of this study is the large cumulative size of alternative haplotype (non-L2E) blocks in the bread wheat D genome. Following hexaploidization, genetic material from the other *Ae. tauschii* lineages (L1 and L3) became incorporated into the bread wheat D genome and were subsequently broken into smaller fragments via recombination. Although the proportions of alternative haplotype blocks are low in individual elite wheat cultivars, the different segments accumulate to considerable lengths across various genotypes. This notion is evidenced by the cumulative size of L3 segments that span a total of 666.0 Mb. We assessed 126 hexaploid wheat landraces, and although we selected for accessions with increased L3 genome content, it is likely that the proportion of remnant L3 segments in the bread wheat gene pool is even higher. This finding raises important questions about the adaptive potential of alternative haplotype blocks for wheat breeding.

Online content

Any methods, additional references, Nature Portfolio reporting summaries, source data, extended data, supplementary information, acknowledgements, peer review information; details of author contributions and competing interests; and statements of data and code availability are available at https://doi.org/10.1038/s41586-024-07808-z.

1. Dubcovsky, J. & Dvorak, J. Genome plasticity a key factor in the success of polyploid wheat under domestication. *Science* **316**, 1862–1866 (2007).
2. Zhou, Y. et al. *Triticum* population sequencing provides insights into wheat adaptation. *Nat. Genet.* **52**, 1412–1422 (2020).
3. Tadesse, W. et al. Genetic gains in wheat breeding and its role in feeding the world. *Crop Breed. Genet. Genom.* **1**, e190005 (2019).
4. Marcussen, T. et al. Ancient hybridizations among the ancestral genomes of bread wheat. *Science* **345**, 1250092 (2014).
5. Wang, J. et al. *Aegilops tauschii* single nucleotide polymorphisms shed light on the origins of wheat D-genome genetic diversity and pinpoint the geographic origin of hexaploid wheat. *New Phytol.* **198**, 925–937 (2013).
6. Zhao, X. et al. Population genomics unravels the Holocene history of bread wheat and its relatives. *Nat. Plants* **9**, 403–419 (2023).
7. Gaut, B. S., Seymour, D. K., Liu, Q. & Zhou, Y. Demography and its effects on genomic variation in crop domestication. *Nat. Plants* **4**, 512–520 (2018).
8. Leal-Bertioli, S. C. et al. Segmental allopolyploidy in action: increasing diversity through polyploid hybridization and homoeologous recombination. *Am. J. Bot.* **105**, 1053–1066 (2018).
9. Cheng, H. et al. Frequent intra- and inter-species introgression shapes the landscape of genetic variation in bread wheat. *Genome Biol.* **20**, 136 (2019).
10. He, F. et al. Exome sequencing highlights the role of wild-relative introgression in shaping the adaptive landscape of the wheat genome. *Nat. Genet.* **51**, 1194–1194 (2019).
11. Walkowiak, S. et al. Multiple wheat genomes reveal global variation in modern breeding. *Nature* **588**, 277–283 (2020).
12. Keilwagen, J. et al. Detecting major introgressions in wheat and their putative origins using coverage analysis. *Sci. Rep.* **12**, 1908 (2022).
13. Ahmed, H. I. et al. Einkorn genomics sheds light on history of the oldest domesticated wheat. *Nature* **620**, 830–838 (2023).
14. Gaurav, K. et al. Population genomic analysis of *Aegilops tauschii* identifies targets for bread wheat improvement. *Nat. Biotechnol.* **40**, 422–431 (2022).
15. Zhou, Y. et al. Introgressing the *Aegilops tauschii* genome into wheat as a basis for cereal improvement. *Nat. Plants* **7**, 774–786 (2021).
16. Wenger, A. M. et al. Accurate circular consensus long-read sequencing improves variant detection and assembly of a human genome. *Nat. Biotechnol.* **37**, 1155–1162 (2019).
17. Manni, M., Berkeley, M. R., Seppey, M., Simão, F. A. & Zdobnov, E. M. BUSCO update: novel and streamlined workflows along with broader and deeper phylogenetic coverage for scoring of eukaryotic, prokaryotic, and viral genomes. *Mol. Biol. Evol.* **38**, 4647–4654 (2021).
18. Lieberman-Aiden, E. et al. Comprehensive mapping of long-range interactions reveals folding principles of the human genome. *Science* **326**, 289–293 (2009).
19. Wang, L. et al. *Aegilops tauschii* genome assembly Aet v5.0 features greater sequence contiguity and improved annotation. *G3* **11**, jkab325 (2021).
20. Zhu, T. et al. Optical maps refine the bread wheat *Triticum aestivum* cv. Chinese Spring genome assembly. *Plant J.* **107**, 303–314 (2021).
21. Mizuno, N., Yamasaki, M., Matsuoka, Y., Kawahara, T. & Takumi, S. Population structure of wild wheat D-genome progenitor *Aegilops tauschii* Coss.: implications for intraspecific lineage diversification and evolution of common wheat. *Mol. Ecol.* **19**, 999–1013 (2010).
22. Savary, S. et al. The global burden of pathogens and pests on major food crops. *Nat. Ecol. Evol.* **3**, 430–439 (2019).
23. Olson, E. L. et al. Simultaneous transfer, introgression, and genomic localization of genes for resistance to stem rust race TTKSK (Ug99) from *Aegilops tauschii* to wheat. *Theor. Appl. Genet.* **126**, 1179–1188 (2013).
24. Periyannan, S. et al. The gene *Sr33*, an ortholog of barley *Mla* genes, encodes resistance to wheat stem rust race Ug99. *Science* **341**, 786–788 (2013).
25. Arora, S. et al. Resistance gene cloning from a wild crop relative by sequence capture and association genetics. *Nat. Biotechnol.* **37**, 139–143 (2019).
26. Boden, S. et al. Updated guidelines for gene nomenclature in wheat. *Theor. Appl. Genet.* **136**, 72 (2023).
27. Raupp, W., Brown-Guedira, G. & Gill, B. Cytogenetic and molecular mapping of the leaf rust resistance gene *Lr39* in wheat. *Theor. Appl. Genet.* **102**, 347–352 (2001).
28. Singh, S. et al. *Lr41*, *Lr39*, and a leaf rust resistance gene from *Aegilops cylindrica* may be allelic and are located on wheat chromosome 2DS. *Theor. Appl. Genet.* **108**, 586–591 (2004).
29. Kolmer, J. A. & Fajolu, O. Virulence phenotypes of the wheat leaf rust pathogen, *Puccinia triticina*, in the United States from 2018 to 2020. *Plant Dis.* **106**, 1723–1729 (2022).
30. Athiyannan, N. *Molecular Genetic Characterisation of Triple Rust Resistance in* Aegilops tauschii. PhD thesis, Univ. of Queensland (2018).
31. Wang, Y. et al. An unusual tandem kinase fusion protein confers leaf rust resistance in wheat. *Nat. Genet.* **55**, 914–920 (2023).
32. Yu, G. et al. The wheat stem rust resistance gene *Sr43* encodes an unusual protein kinase. *Nat. Genet.* **55**, 921–926 (2023).

33. Klymiuk, V., Coaker, G., Fahima, T. & Pozniak, C. J. Tandem protein kinases emerge as new regulators of plant immunity. *Mol. Plant Microbe Interact.* **34**, 1094–1102 (2021).
34. Athiyannan, N. et al. Long-read genome sequencing of bread wheat facilitates disease resistance gene cloning. *Nat. Genet.* **54**, 227–231 (2022).
35. Sansaloni, C. et al. Diversity analysis of 80,000 wheat accessions reveals consequences and opportunities of selection footprints. *Nat. Commun.* **11**, 4572 (2020).
36. Beridze, R. K., Hanelt, P., Kandelaki, V. N., Sakvarelidze, I. M. & Schultze-Motel, J. A further mission to the Georgian SSR 1984 for collecting indigenous material of cultivated plants. *Kulturpflanze* **33**, 199–212 (1985).
37. Rosyara, U. et al. Genetic contribution of synthetic hexaploid wheat to CIMMYT's spring bread wheat breeding germplasm. *Sci. Rep.* **9**, 12355 (2019).
38. Cheng, S. et al. Harnessing landrace diversity empowers wheat breeding. *Nature* https://doi.org/10.1038/s41586-024-07682-9 (2024).
39. Delorean, E. et al. High molecular weight glutenin gene diversity in *Aegilops tauschii* demonstrates unique origin of superior wheat quality. *Commun. Biol.* **4**, 1242 (2021).
40. Sato, K. et al. Chromosome-scale genome assembly of the transformation-amenable common wheat cultivar 'Fielder'. *DNA Res.* **28**, dsab008 (2021).
41. Kale, S. M. et al. A catalogue of resistance gene homologs and a chromosome-scale reference sequence support resistance gene mapping in winter wheat. *Plant Biotechnol. J.* **20**, 1730–1742 (2022).
42. Wang, Z. Y. et al. Helitron and CACTA DNA transposons actively reshape the common wheat-AK58 genome. *Genomics* **114**, 110288 (2022).
43. Guo, W. et al. Origin and adaptation to high altitude of Tibetan semi-wild wheat. *Nat. Commun.* **11**, 5085 (2020).
44. Gonçalves-Dias, J., Singh, A., Graf, C. & Stetter, M. G. Genetic incompatibilities and evolutionary rescue by wild relatives shaped grain amaranth domestication. *Mol. Biol. Evol.* **40**, msad177 (2023).
45. Weide, A., Riehl, S., Zeidi, M. & Conard, N. J. A systematic review of wild grass exploitation in relation to emerging cereal cultivation throughout the Epipalaeolithic and aceramic Neolithic of the Fertile Crescent. *PLoS ONE* **13**, e0189811 (2018).
46. Singh, N. et al. Genomic analysis confirms population structure and identifies inter-lineage hybrids in *Aegilops tauschii*. *Front. Plant Sci.* **10**, 9 (2019).

[1]Plant Science Program, Biological and Environmental Science and Engineering Division (BESE), King Abdullah University of Science and Technology (KAUST), Thuwal, Saudi Arabia. [2]Faculty of Land and Food Systems, The University of British Columbia (UBC), Vancouver, British Columbia, Canada. [3]Computer, Electrical and Mathematical Sciences and Engineering Division (CEMSE), Computational Bioscience Research Center (CBRC), King Abdullah University of Science and Technology (KAUST), Thuwal, Saudi Arabia. [4]John Innes Centre, Norwich Research Park, Norwich, UK. [5]Institute of Molecular Biology and Biotechnologies, Ministry of Science and Education of the Republic of Azerbaijan, Baku, Azerbaijan. [6]Wheat Research Department, Field Crops Research Institute, Agricultural Research Center (ARC), Giza, Egypt. [7]Department of Agroecology, Aarhus University, Slagelse, Denmark. [8]Department of Plant Sciences, Quaid-i-Azam University, Islamabad, Pakistan. [9]International Maize and Wheat Improvement Centre (CIMMYT), c/o CAAS, Beijing, China. [10]State Key Laboratory of Crop Gene Resources and Breeding and National Key Facility for Crop Gene Resources and Genetic Improvement, Institute of Crop Science, Chinese Academy of Agricultural Sciences, Beijing, China. [11]Commonwealth Scientific and Industrial Research Organization (CSIRO), Agriculture and Food, Canberra, New South Wales, Australia. [12]Institute for Cereal Crops Improvement, School of Plant Sciences and Food Security, Tel Aviv University, Tel Aviv, Israel. [13]Leibniz Institute of Plant Genetics and Crop Plant Research (IPK), Seeland, Germany. [14]German Centre for Integrative Biodiversity Research (iDiv) Halle-Jena-Leipzig, Leipzig, Germany. [15]Institute of Agricultural and Nutritional Sciences, Martin Luther University Halle-Wittenberg, Halle, Germany. [16]Julius Kuehn-Institute (JKI), Federal Research Centre for Cultivated Plants, Institute for Resistance Research and Stress Tolerance, Quedlinburg, Germany. [17]Bioscience Core Lab, King Abdullah University of Science and Technology (KAUST), Thuwal, Saudi Arabia. [18]Department of Plant Pathology, Kansas State University, Manhattan, KS, USA. [19]Department of Plant Pathology and Wheat Genetics Resource Center, Kansas State University, Manhattan, KS, USA. [20]Department of Plant, Soil and Microbial Sciences, Michigan State University, East Lansing, MI, USA. [21]National Institute of Agricultural Sciences, Rural Development Administration, Jeonju, South Korea. [22]School of Agricultural Biotechnology, Punjab Agricultural University, Ludhiana, India. [23]Plant Breeding Institute, School of Life and Environmental Sciences, University of Sydney, Cobbitty, New South Wales, Australia. [24]Triticeae Research Institute, Sichuan Agricultural University, Chengdu, China. [25]Department of Biology and Microbiology, South Dakota State University, Brookings, SD, USA. [26]Institute of Botany, Plant Physiology and Genetics, Tajik National Academy of Sciences, Dushanbe, Tajikistan. [27]Department of Plant Sciences, University of California, Davis, CA, USA. [28]Department of Plant Sciences, University of the Free State, Bloemfontein, South Africa. [29]Department of Plant Pathology, University of Minnesota, Saint Paul, MN, USA. [30]Department of Plant Science and Landscape Architecture, University of Maryland, College Park, MD, USA. [31]Nottingham Wheat Research Centre, School of Biosciences, University of Nottingham, Loughborough, UK. [32]University of Saskatchewan, Crop Development Centre, Agriculture Building, Saskatoon, Saskatchewan, Canada. [33]Ecology and Evolutionary Biology, School of Biosciences, University of Sheffield, Western Bank, Sheffield, UK. [34]Cereal Disease Laboratory, USDA-ARS, St Paul, MN, USA. [35]Crop Improvement and Genetics Research Unit, Western Regional Research Center, USDA-ARS, Albany, CA, USA. [36]Peanut and Small Grains Research Unit, USDA-ARS, Stillwater, OK, USA. [37]Present address: Centre for Crop Health School of Agriculture and Environmental Science, University of Southern Queensland, Toowoomba, Queensland, Australia. [38]Present address: Centre d'anthropobiologie et de génomique de Toulouse (CAGT), Laboratoire d'Anthropobiologie et d'Imagerie de Synthèse, CNRS UMR 5288, Faculté de Médecine de Purpan, Toulouse, France. [39]Present address: National Key Laboratory of Plant Molecular Genetics, Center for Excellence in Molecular Plant Sciences, Institute of Plant Physiology and Ecology, Chinese Academy of Sciences, Shanghai, China. [40]Present address: Department of Plant Science, University of Manitoba, Winnipeg, Manitoba, Canada. [41]Present address: Faculty of Agricultural, Life and Environmental Sciences, University of Alberta, Edmonton, Canada. [42]These authors contributed equally: Emile Cavalet-Giorsa, Andrea González-Muñoz, Naveenkumar Athiyannan. ✉e-mail: brande.wulff@kaust.edu.sa; simon.krattinger@kaust.edu.sa

Methods

Establishing *Ae. tauschii* genomic resources

Plant material. We compiled a database comprising 1,124 *Ae. tauschii* accessions with associated passport data in Supplementary Table 1 (Supplementary Note 1). Duplicate germplasm bank IDs were identified and passport data collated using the Plant Genetic Resources for Food and Agriculture (PGRFA) database (https://www.genesys-pgr.org/) or other sources as indicated in Supplementary Table 1. From this database, seed of 228 non-redundant accessions were obtained from the Open Wild Wheat Consortium *Ae. tauschii* Diversity Panel collection deposited at the Germplasm Resource Unit (GRU) of the John Innes Centre; 48 accessions from the Cereal Crop Wild Relatives (*Triticeae*) collection of the GRU; 19 accessions from the Designing Future Wheat (DFW) Wheat Academic Toolkit collection of the GRU that have been used as synthetic hexaploid wheat D genome donors; 223 accessions from the Wheat Genetics Resource Center (WGRC) of Kansas State University; 34 accessions from the Plant Gene Resources of Canada (PGRC); 84 accessions donated by the Institute of Botany, Plant Physiology and Genetics of the Tajikistan National Academy of Sciences; 20 accessions donated by the Azerbaijan National Academy of Sciences; and 37 accessions donated by Quaid-i-Azam University. Accession P-99.95-1.1 was obtained from the Deposited Published Research Material collection of the GRU.

We also resequenced and analysed 60 hexaploid wheat landraces. The list can be found in Supplementary Table 14. Out of the 60 wheat landraces, 57 were received from the International Maize and Wheat Improvement Center (CIMMYT) and 3 were from the International Center for Agricultural Research in the Dry Areas (ICARDA).

Re-sequencing of *Ae. tauschii* and hexaploid wheat accessions. In this study, we generated short-read WGS data for 350 *Ae. tauschii* accessions (Supplementary Table 1) and 59 hexaploid wheat accessions (Supplementary Table 14). We isolated DNA following the CTAB protocol described by Abrouk et al.[47] from leaf tissue of 2-week-old seedlings under prior dark treatment for 48 h. DNA was quantified using the Qubit dsDNA HS Assay (Thermo Fisher Scientific) and purity was determined according to 260/280 and 260/230 absorbance ratios using a Nanodrop spectrophotometer. PCR-free paired-end libraries were constructed and sequenced on an Illumina Novaseq 6000 instrument, yielding a median 8.3-fold coverage per sample (ranging from 5.87- to 16.86-fold) for the *Ae. tauschii* samples and a minimum tenfold coverage for the bread wheat samples (Supplementary Tables 1 and 14). Library preparation and sequencing was performed as a service by Novogene.

Library construction and RNA sequencing. Seedlings of *Ae. tauschii* accessions TA10171, TA1675 and TA2576 were raised as 5–6 seeds per pot (6 × 6 × 10 cm) in a growth chamber at 22–24 °C under long-day photoperiods of 16/8 h day/night cycle with high-output white-fluorescent tubes until the third leaf stage (about 2–3 weeks old), and then transferred to a 4 °C growth chamber with a long-day photoperiod for vernalization. After a nine-week vernalization period, all the plants were moved back to the original growth chamber under the controlled conditions mentioned above. In total, 45 tissue samples were collected: From each of the three accessions, three biological replicates were taken from each of: young leaf, root, stem, flag leaf and inflorescence. Samples were collected at the same time of day at approximately 5–6 h after daylight. The seedling leaves and roots were harvested after two weeks of recovery in the original growth chamber and rinsed with water to remove soil particles. When the plants had 4–5 tillers, the stems, flag leaves and inflorescences were harvested together. The green inflorescences were collected immediately after pollination. The 5-cm-long stem sections and youngest flag leaves were measured from the top of the same inflorescences. Samples were placed in liquid nitrogen after harvest and stored at −80 °C.

The samples were ground into a fine powder in liquid nitrogen in a ceramic mortar and pestle to isolate RNA using the Qiagen RNeasy Mini Kit following the manufacturer's protocol. The quality of RNA was determined on a 1% agarose gel, and RNA concentration was measured using a NanoPhotometer (Implen) at 260 nm and 280 nm. Sample collection time and relative details are listed in Supplementary Table 23. High-quality RNA samples were delivered for RNA integrity test, poly-A mRNA enrichment, library construction and PE100 sequencing using the Illumina NovaSeq system (Génome Québec, Canada).

PacBio HiFi genome sequencing; primary assembly of the *Ae. tauschii* genomes and CWI 86942. We selected 46 *Ae. tauschii* accessions, including 11 L1 accessions, 34 L2 accessions and 1 L3 accession. These 46 accessions were selected to span the geographical range of the species (Fig. 1a) and provide a collection of phenotypes related to disease and pest resistance, abiotic tolerance and agromorphological traits of strategic interest to the Open Wild Wheat Consortium for bread wheat improvement (Supplementary Table 4). We included a higher proportion of accessions from L2 relative to L1 based on reported phylogenies showing that L2 is more genetically diverse than L1[5,14,21]. A single L3 accession was selected based on low genetic diversity observed among five non-redundant L3 accessions in the phylogeny reported by Gaurav et al.[14]. Several accessions were selected to maximize the genetic diversity based on a core subset sampling analysis using Core Hunter (v3)[48], using the 'average entry-to-nearest-entry' distance measure, aiming to maximally represent the diversity of the panel of 242 non-redundant accessions published by Gaurav et al.[14]. The bread wheat landrace CWI 86942 was selected based on a high L3 *k*-mer content.

For the *Ae. tauschii* accessions, 'high molecular weight' genomic DNA was isolated from leaf tissue of three to four-week-old dark-treated seedlings. We followed the high molecular weight DNA isolation protocol optimized by Driguez et al.[49] for long-read sequencing. DNA integrity was confirmed using the FemtoPulse system (Agilent). DNA was quantified using the Qubit dsDNA HS Assay (Thermo Fisher Scientific) and purity was determined according to 260/280 and 260/230 ratios using a Nanodrop spectrophotometer. For the bread wheat accession CWI 86942, leaves from two-week old seedlings were collected from two different plants and high molecular weight DNA extraction was performed as mentioned above[49]. All the library preparation and Circular Consensus Sequencing (CCS) was performed on a PacBio Sequel II instrument, as a service by Novogene.

For *Ae. tauschii*, HiFi reads were assembled using hifiasm (v0.16.1)[50] with parameters "-l0 -u -f38" optimized for homozygous and large genomes (-l0 -f38) and to minimize misassemblies by disabling the post-join contigs step (-u), favouring accuracy over contiguity. Sequencing coverage ranged from 18 to 47-fold depending on the accession, except for the three *Ae. tauschii* lineage reference accessions (TA10171, TA1675 and TA2576) for which the coverage was increased to 67 - 97-fold. For assembly validation and quality control, we used QUAST (v5.0.2)[51] to calculate the assembly metrics, Merqury (v1.3)[52] to estimate the base-call accuracy and *k*-mer completeness based on 21-mer produced from the short-read WGS data[14] and BUSCO (v5.3.1)[17] with the embryophyta_odb10 database to determine the completeness of each genome assembly. The number of homozygous SNPs and short insertion–deletion mutations (indels) was determined comparing the HiFi assemblies against the respective WGS data (Supplementary Table 24). They are in the range of 3,416–40,885 homozygous SNPs or indels per accession.

For CWI 86942, we performed the primary contig-level assembly with 484.33 Gb of HiFi reads (32-fold coverage) using the LJA assembler (v0.2)[53] with default parameters. Assembly metrics and QC were performed with QUAST (v5.0.2)[51] and BUSCO (v5.3.1)[17] with the embryophyta_odb10 database.

Chromosome conformation capture sequencing and chromosome-scale scaffolding. In situ Hi-C libraries were prepared for TA1675 and TA10171 from two-week-old *Ae. tauschii* plants according to the previously published protocol[54]. Libraries were quantified and sequenced (paired-end, 2 ×111 cycles) using the Illumina NovaSeq 6000 device (Illumina) at IPK Gatersleben[55], yielding 316 million paired-end reads (150 bp) for TA1675 and 215 million paired-end reads for TA10171.

For TA2576, two-week-old, dark-treated leaf tissue samples were harvested and cross-linked with formaldehyde for library preparation and Hi-C sequencing by Phase Genomics, yielding 543 million paired-end reads (150 bp). For CWI 86942, two Omni-C libraries were generated and sequenced from two-week-old, dark-treated leaf tissue samples as a service by Dovetail Genomics. The total yield was 715 million paired-end reads (150 bp).

Scaffolding into pseudomolecules for TA10171, TA1675, TA2576 and CWI 86942 was performed from their primary assemblies and their specific Hi-C and Omni-C data, respectively. Hi-C and Omni-C reads were processed with Juicer (v1.6)[56] (for the Hi-C reads, parameter: -s DpnII) to convert raw fastq reads to chromatin contacts and remove duplicates. The chromatin contacts were used to scaffold the contig-level assemblies using 3D-DNA (v190716)[57] (using run-asm-pipeline.sh with -r 0 parameter). Scaffolds were visualized, manually oriented and ordered using Juicebox (v2.20.00)[58].

RagTag assembly of 43 *Ae. tauschii* accessions. The remaining 43 contig-level assemblies were scaffolded into chromosome-scale assemblies using RagTag (v2.1.0)[59] and the three high-quality genomes (TA10171, TA1675 and TA2576) as anchors. In brief, the primary contig-level assemblies were scaffolded using RagTag scaffold against the respective chromosome-scale reference assemblies generated in this study. After running RagTag scaffold, the placed contigs had the exact same lengths as the primary contigs before running RagTag scaffold. Also, the number of gaps in each RagTag assembly corresponds to the number of placed contigs minus seven (number of chromosomes) (Supplementary Table 6). This indicates that RagTag scaffold did not introduce misassemblies or duplicated contig ends. The scaffolded assemblies were validated with dot-plots generated using MashMap (v3.0.6)[60] against the corresponding reference assembly. While being great resources for gene discovery and comparative analyses, reference-guided assemblies are limited in their ability to study large structural rearrangements.

Repeat and gene annotation. Paired-end RNA-seq reads for TA10171, TA1675 and TA2576 were first cleaned using Trimmomatic (v0.40)[61] with the following settings "ILLUMINACLIP:TruSeq3-PE.fa:2:30:10:2:True LEADING:30 TRAILING:30 MINLEN:36". Trimmed paired-end reads were aligned to the corresponding genome assembly using STAR (v2.7.10b)[62] with the parameters "--twopassMode basic --outFilterMismatchNMax 5 --outFilterMatchNminOverLread 0.80 --alignMatesGapMax 100000 --outSAMstrandField intronMotif --runMode alignReads" and the results were filtered and sorted using SAMtools (v1.10)[63]. Then, the BRAKER (v3.0.3)[64–66] pipeline was used to predict de novo gene models using RNA-Seq and protein data mode with the *Viridiplantae* protein models provided by OrthoDB (v11). Predicted gene annotations obtained from BRAKER were processed using a combination of NCBI BLAST+ (v2.9.0-2)[67], AGAT (v1.2.1) (https://github.com/NBISweden/AGAT), InterProScan (v5.64-96.0)[68,69], and R (v4.2.0). Outputs from BRAKER3 were first converted to gff3 and CDS and protein sequences were extracted using "agat_sp_extract_sequences.pl" from AGAT package. BLASTn was used to perform a reciprocal BLAST of the predicted CDS against themselves, and a unidirectional BLAST against the Ensembl nrTEplantsJune2020.fa repetitive elements database, using default search parameters. The putative functions for each annotated gene model were predicted using InterProScan with default parameters for the following databases: FunFam, SFLD, PANTHER, Gene3D, PRINTS, Coils, SUPERFAMILY, SMART, CDD, PIRSR, ProSitePatterns, AntiFam, Pfam, MobiDBLite, PIRSF, NCBIfam. R (v4.2.0) (in R studio) was used to visualize and filter these results. Predicted transcripts with fewer than 50 exact and fewer than 150 inexact self-BLAST results were retained. Predicted transcripts were retained from the final de novo annotation if there were (1) no exact matches to the transposable elements database, and (2) at least one domain predicted by any of: FunFam, PANTHER, Gene3D, SUPERFAMILY, ProSitePatterns, Pfam, CDD, InterPro. Predicted genes were considered as 'low confidence' if there were no exact matches to the database of original transcript predictions. The remaining annotated genes were considered as 'high confidence'. Validation and annotation completeness was performed using agat_sp_statistics.pl and BUSCO (v5.4.7)[17] running in transcriptome mode with the poales_odb10 database. We used OrthoFinder[70] (v2.5.4) with default parameters to perform gene family analysis.

Repeat annotation was performed using RepeatMasker (v4.1.2-p1)[71] and the Ensembl nrTEplantsJune2020 repetitive elements database[72] using the RMBlast engine.

For bread wheat accession CWI 86942, gene model prediction was performed using a lifting approach similarly to the one described in Abrouk et al.[73] with a combination of liftoff (v1.6.3)[74], AGAT and gffread (v0.11.7)[75]. In brief, gene model annotations of hexaploid wheat line Chinese Spring, Kariega, Fielder, Arina*LrFor*, Julius and Norin61 were independently transferred using liftoff (parameters: -a 0.9 -s 0.9 -copies -exclude_partial -polish) and all the output gff files were merged into a single file using the Perl script agat_sp_merge_annotations.pl. The merged file was then post-processed using gffread tools (parameters: --keep-genes -N -J) to retain transcripts with start and stop codons, and to discard transcripts with (1) premature stop codons, and/or (2) having introns with non-canonical splice sites. In total, 147,646 gene models were predicted for which the putative functional annotations were assigned using a protein comparison against the UniProt database (2021_03) using DIAMOND (v2.1.8)[76] (parameters: -f 6 -k1 -e 1e-6). PFAM domain signatures and GO were assigned using InterproScan (v5.55-88.09)[68,69]. The BUSCO score showed a completeness of 99.2% (96.4% duplicated) with the poales_odb10 database[17].

k-mer matrix generation, redundancy and diversity analyses

***k*-mer matrix generation.** We developed an optimized *k*-mer matrix workflow to generate a presence/absence *k*-mer matrix for large diversity panels (Supplementary Note 2) (https://github.com/githubcbrc/KGWASMatrix). We counted *k*-mers ($k = 51$) in raw sequencing data for 350 accessions generated in this study, 306 accessions published by Gaurav et al.[14], 275 accessions published by Zhou et al.[15] and 24 accessions by Zhao et al.[6]. The 35 accessions with less than fivefold sequencing coverage were discarded to avoid affecting the *k*-mer count. *k*-mers with a count of one were discarded prior to generating the *k*-mer matrix. *k*-mers were retained in the *k*-mer matrix by a minimum occurrence of 6 across accessions and a maximum occurrence of ($N - 6$), where N is the total number of accessions.

Redundancy analysis. A redundancy analysis was performed using a subset of 100,000 random *k*-mers sampled from the *k*-mer matrix of 920 *Ae. tauschii* accessions. The complete matrix contained 10,078,115,665 *k*-mers. The pairwise comparisons between accessions were performed by computing the sum of the presence–absence values (0 and 1) per *k*-mer between 2 accessions of the matrix. To determine the divergence, we computed the total number of 1 present in the summed string, each one corresponding to a difference in the presence/absence of the *k*-mer in the 2 compared accessions. In the sum, the presence of a *k*-mer in two accessions would result in a 2 and the absence in both accessions in a 0. A threshold of 96% shared *k*-mers was used to call redundancy based on control lines determined by Gaurav et al.[14] to be genetically redundant based on a SNP analysis.

Estimation of the genetic diversity in the 46 *Ae. tauschii* accessions selected for high-quality genome assemblies. We computed the *k*-mer accumulation across the 46 *Ae. tauschii* accessions by analysing their *k*-mer presence or absence in the *k*-mer matrix. First, we extracted a *k*-mer sub-matrix for the 46 accessions and removed *k*-mers that were absent from all accessions. The *k*-mer accumulation was computed by counting the number of *k*-mers present in the first accession, then adding new *k*-mers from the second accession (that is, not present in the previous accession) and sequentially adding new *k*-mers until accession 46. This computation was iterated 100 times using randomly shuffled sub-matrices, and the mean and standard deviation were calculated. The mean cumulative *k*-mer counts were fitted to a logarithmic function ($y = a + b \times \log(x)$] using the Python function optimize.curve_fit from SciPy library (v1.8.0)[77]. The fitted data were plotted using the Python seaborn library (v0.11.2)[78] to visualize the *k*-mer-based accumulation curve. We calculated the *k*-mer frequency across the full panel of 920 *Ae. tauschii* accessions in comparison to the genetic diversity in the 46 accessions. The *k*-mers were divided into two groups: *k*-mers present and absent in the 46 accessions. We extracted *k*-mer sub-matrices for each group and computed the occurrence of the *k*-mers across the 920 accessions (Extended Data Fig. 1c). We plotted the square root transformation of the *k*-mer frequency using the Python seaborn library (v0.11.2)[78].

SNP calling. Fastq raw reads were trimmed using Trimmomatic (v0.38)[61] with the following settings "ILLUMINACLIP:adapters.fa:2:30:10 LEADING:3 TRAILING:3 SLIDINGWINDOW:4:15 MINLEN:36". Cleaned reads were mapped on the TA1675 assembly using BWA mem (v0.7.17)[79] and sorted with SAMtools (v1.8)[63]. Variants were called using BCFtools mpileup (v1.9)[63] with the setting "-C 60 -q 5 -Q 20", and only SNPs were retained as variants. The filtering was performed using BCFtools, retaining only sites with a maximum depth of 40, a quality higher than 100 and an allele count higher than 1. For quality check, we counted the percentage of divergent sites using re-sequencing data from TA1675 against the chromosome-scale TA1675 reference assembly, revealing an error rate of 0.18%. For the assessment of assembly quality (Supplementary Table 24), homozygous indels were also retained (maximum number of raw reads supporting an indel (IDV) = 3, maximum fraction of raw reads supporting an indel (IMF) = 0.3, depth between 5 and 40, a quality higher than 30 and an allele count higher than one). We further computed the SNP density across the chromosomes and calculated allele frequency (Extended Data Fig. 8a–c and Supplementary Tables 25–27). In total, 957 *Ae. tauschii* and 59 wheat landraces accessions reached the quality threshold of a coverage higher than fivefold after trimming and were used for SNP calling. The SNP data set was used for phylogenetic, ancestry, and nucleotide diversity analyses.

The phylogenetic tree was built from the filtered SNPs using vcfkit (v0.1.6)[80] with the UPGMA algorithm. Ancestry analysis was performed using the sNMF (Fast and Efficient Estimation of Individual Ancestry Coefficients) approach available in the LEA R package (v3.10.2)[81]. For each run, we performed 20 repetitions using the following parameters "alpha = 10, tolerance = 0.00001, iterations = 300" up to $K = 28$. Supplementary Table 28 shows the minimum cross-entropy values for 20 sNMF runs across different values of K.

We estimated the nucleotide diversity (π) in the 493 non-redundant accession of *Ae. tauschii* using the filtered SNP calls against the TA1675 reference assembly. We calculated π over 10-kb windows of the genome using VCFtools (v0.1.16)[82] (parameter --window-pi 10000).

Structural variant calling. We determined the structural variation across the 46 high-quality assemblies with reference to the chromosome-scale assembly of TA1675. Structural variants of >50 bp in length and up to 100 kb were called using the PacBio structural variant calling and analysis suite (pbsv) (v2.9.0) and following the pipeline described at (https://github.com/PacificBiosciences/pbsv). In brief, HiFi sequencing reads in bam format were aligned to the reference genome using pbmm2 aligner (v1.10.0) (https://github.com/PacificBiosciences/pbmm2). The bam file was indexed as CSI suitable for larger genomes. Signatures of structural variation were detected and structural variants were called per accession in vcf format, then concatenated into a single bed file per lineage.

The *Ae. tauschii* genomes facilitate gene discovery

***k*-mer-based genome-wide association in *Ae. tauschii*.** We followed the *k*-mer GWAS (*k*GWAS) pipeline described by Gaurav et al.[14] using the Python scripts available at (https://github.com/wheatgenetics/owwc/tree/master/kGWAS) and the phenotype data for stem rust and leaf rust available for this panel to specifically run the association mapping and plotting using default parameters. The association mapping analyses showing the effect of assembly quality in *Ae. tauschii* accession TA1662 were performed using previously published phenotype data for reaction to *Pgt* race QTHJC[14]. The *k*GWAS for leaf rust to identify *Lr39* in *Ae. tauschii* accession TA1675 was performed using phenotype data for reaction to *Pt* race BBBDB (Supplementary Table 29).

***SrTA1662* haplotype analysis.** To identify the *SrTA1662* locus in the contig-level assembly of *Ae. tauschii* accession TA1662, we performed a BLASTn (v2.12.0)[67] search of the *SrTA1662* gene sequence (GenBank ID MW526949.1) published by Gaurav et al.[14]. To identify the *SR33* locus in the contig-level assembly of *Ae. tauschii* accession CPI 110799 (the original source of *Sr33*), we searched for the *RGA1e* (also known as *Sr33*) gene sequence (GenBank ID KF031291.1) published by Periyannan et al.[24]. *RGA1e* gene sequences were also searched against the contig-level assemblies of accessions AUS 18911 (KF031299.1) and AUS 18913 (KF031284.1)[24]. For all accessions, the genes were found within a single contig that located to the chromosome arm 1DS based on the scaffolding against the TA1675 reference assembly. In the four accessions, we performed BLASTn searches for additional *Ae. tauschii* resistance gene analogues (*RGA1a-d*, *RGA2a-b*, *RGA3a*) reported by Periyannan et al.[24] (GenBank ID KF031285.1–KF031299.1). To confirm that this region is orthologous to the *Mla* locus in barley, we searched for the presence of the pumilio (*Bpm*) gene homologue and subtilisin-chymotrypsin inhibitor (*CI*) genes in gene-lifting annotations for AUS 18911, AUS 18913, CPI 110799 and TA1662. *Bpm* and *CI* genes were previously reported flanking Resistance Gene Homologues (RGH) of the *Mla* locus[83]. The gene-lifting annotations were generated using liftoff v1.6.1[74] with default parameters based on the TA1675 genome annotation.

Phylogenetic analysis of RGAs in *Ae. tauschii*. To provide further evidence for the homology of the *SrTA1662* (*SR66*) and *SR33* loci in *Ae. tauschii* and the *Mla* locus in barley, we performed phylogenetic analyses of RGA and RGH gene sequences. Clustal algorithm with default parameters was used for the DNA sequence multiple alignment. We used the unweighted UPGMA algorithm with bootstrap testing to support the tree topology with 5,000 replicates. The phylogenetic analyses were performed using MEGA (v11)[84,85].

Leaf rust inoculations and association studies. The evaluation of resistance and susceptibility in 149 *Ae. tauschii* L2 accessions was conducted against the North American *Pt* race isolate BBBDB 1-1[86] using seedlings organized in cone racks. Every cone rack housed 98 cones, and each cone was sown with three seeds. The primary leaves of seedlings, aged 8–9 days, were subjected to inoculation by distributing 1 ml of inoculum per cone rack, which consisted of 15 mg of spores in 1 ml of Soltrol 170 (Chevron Phillips Chemical Company). The delivery to each plant was 0.05 mg of urediniospores. Post-inoculation, the phytotoxicity from the oil carrier, Soltrol 170, was mitigated by mildly fanning the leaves for 2 h under the illumination of 400-Watt HPS bulbs to expedite the evaporation of the carrier oil. The seedlings, once inoculated, were placed in mist chambers maintained at 22 °C, where 100% humidity was sustained using a domestic ultrasonic humidifier for a period of 16–18 h in the absence of light. Subsequently, the seedlings were transferred to a greenhouse with a 16-h day cycle, maintaining nocturnal and diurnal temperatures at 15 °C and 20 °C, respectively. The phenotypic assessment of disease was undertaken at 10 and 12 dpi using an infection type scoring range of 0 to 3 + , as standardized by Long and Kolmer[87], and depicted as the mean of three individual replicates per accession (Supplementary Table 29).

For use in GWAS, the qualitative scores were converted to a quantitative score by assigning numerical values to the infection types. This was achieved by the *k*GWAS pipeline (https://github.com/wheatgenetics/owwc/tree/master/kGWAS) that performs Stakman IT to numeric scale 1 conversion (RunAssociation_GLM.py with -st parameter).

Bi-parental mapping of *LR39* and candidate gene identification. An *Ae. tauschii* bi-parental mapping population ($n = 123$) was generated by crossing the leaf rust resistant *Ae. tauschii* accession CPI 110672 (synonymous TA1675) with the leaf rust susceptible accession CPI 110717. The mapping population was segregating for a single dominant leaf rust resistance gene ($P = 0.606$) when inoculated with the Australian *Pt* isolate 26-1,3 (PBI culture no 316) and phenotyped at the Plant Breeding Institute, Cobbitty[30]. Bulk segregant analysis of selected homozygous resistant and susceptible F_2 progenies with the 90 K SNP array[88] placed the leaf rust resistance locus to chromosome 2DS. The mapping population was further genotyped with markers derived from the 90 K iSelect SNP array, the TA1675 genomic sequence, and a marker closely linked to *LR39* (*Xgdm35*) (Supplementary Table 30 and 31)[28,89]. Linkage analysis was performed using MapDisto (v2.0)[90] with default parameters such as LOD (logarithm of the odds) threshold of 3.0, maximum recombination frequency of 0.3 and removal of loci with 10% missing data. Genetic distances were calculated using the Kosambi mapping function, and the map was created using MapChart (v2.32)[91]. Markers flanking *LR39* were anchored to the TA1675 reference assembly. Annotated high-confidence genes at the delimited physical interval were screened for protein homology using BLASTp to identify diversity between TA1675 and AL8/78 (Supplementary Table 13). The conserved domains and critical residues of WTK and NLR were identified using the amino acid sequences in the NCBI Conserved Domain search (https://www.ncbi.nlm.nih.gov/Structure/cdd/wrpsb.cgi) and InterPro (https://www.ebi.ac.uk/interpro/search/sequence/) databases. The polymorphic SNP corresponding to R457I in WTK was converted to a KASP marker diagnostic for *Lr39* (Supplementary Table 31).

Virus-induced gene silencing. To develop candidate gene-specific VIGS probes, the predicted coding sequences of candidate genes were searched against the TA1675 transcriptome database using siRNA-Finder (siFi21) software (v1.2.3-0008)[92]. Based on the RNA interference (RNAi) design plot, regions predicted to have a higher number of efficient probes and fewer off-targets were used for designing silencing probes for the WTK (LrSi2:258 bp, LrSi6:254 bp and LrSi7:248 bp) and the NLR (LrSi3:234 bp and LrSi8:257 bp) candidate genes. The silencing probe sequences were verified for specificity using a BLAST search against the TA1675 reference assembly (<80% sequence identity for hits other than the target candidate). Designed probes were flanked by XbaI and ApaI and synthesized at GenScript Biotech followed by cloning into the BSMV-γ vector in an antisense direction. The resulting constructs were transformed into *Agrobacterium tumefaciens* strain GV3101. The *Agrobacterium* clones were grown overnight at 28 °C in lysogeny broth with appropriate antibiotics. Cells were collected by centrifugation at 3,500*g* for 10 min, then re-suspended using infiltration buffer (10 mM $MgCl_2$, 10 mM MES pH 6.5 with KOH buffer and 150 mM acetosyringone) and adjusted to an OD_{600} of 1.0 followed by incubation at 28 °C for 3 h. Equal volumes of BSMV-α and BSMV-β were mixed with respective BSMV-γ silencing probes or BSMV-γGFP and infiltrated into *Nicotiana benthamiana* leaves. Infiltrated leaves were collected 5 days after infiltration and homogenized with virus inoculation buffer (10 mM monopotassium phosphate containing 1% Celite (Thermo Fisher Scientific, 68855-54-9)). The homogenate containing viral particles was rub inoculated onto five to ten seedlings of TA1675 at the three leaf stage. After two weeks of recovery and viral symptoms appearing, the seedlings were inoculated with *Pt* isolate B9414. Prior to inoculating TA1675, *Pt* isolate B9414 was propagated on seedlings of the susceptible wheat cultivar Thatcher. Freshly collected urediniospores were suspended in Isopar L and sprayed onto plants using a high-pressure air sprayer. After inoculation, plants were placed in the dark overnight in an incubation box equipped with a humidifier and then transferred to a growth chamber with a 16/8 h day/night cycle, with 21 °C/18 °C growth conditions. Leaf rust phenotypes were recorded at 12 days after inoculation by scanning the leaves at 600 dots per inch on an Epson Perfection V850 Pro scanner. For leaf rust biomass quantification, DNA was extracted from *Pt*-inoculated leaves using the CTAB method[47]. DNA concentrations were measured using a NanoDrop 2000 spectrophotometer (Thermo Fisher Scientific). A 20 µl qPCR reaction containing Power SYBR Green PCR Mix (Applied Biosystems 4367659), ~25 ng of DNA, and primers specific to the *Puccinia* 28 S large subunit or the internal transcribed spacer region[93] and Triticeae elongation factor-specific primers[94] was run using the ABI QuantStudio 6 Flex Real-Time PCR machine. The $2^{-\Delta\Delta CT}$ method was used to normalize rust gene amplification values relative to the *Ae. tauschii* elongation factor endogenous control.

PCR conditions. A 20 µl PCR containing 100 ng of genomic DNA, 1X GoTaq Flexi green buffer, 1.5 mM $MgCl_2$, 200 µM dNTP, 200 nM primers and 1 unit of Taq polymerase (M829B, Promega) was used for various fragment amplifications. Primer sequences are shown in Supplementary Table 31. A touchdown PCR protocol was used as follows: initial denaturation at 94 °C for 30 s; annealing at 65 °C for 30 s, decreasing by 1 °C per cycle; and extension at 72 °C for 60 s, followed by repeating these steps for 14 cycles. After enrichment, the program continued for 29 cycles as follows: 94 °C for 30 s, 58 °C for 30 s, and 72 °C for 60 s. PCR products of cleaved amplified polymorphic sequence (CAPS) markers were digested with appropriate restriction enzymes by following the manufacturer's instructions. A 5 µl reaction (2.5 µl of KASP Master Mix (Low ROX KBS-1016-016), 0.07 µl of assay mix and 2.5 µl (25 ng) of DNA) was used for KASP markers. PCR cycling was performed in an ABI QuantStudio 6 Flex Real-Time PCR machine as follows: preread at 30 °C for 60 s; hold stage at 94 °C for 15 min; and then ten touchdown cycles (94 °C for 20 s; touchdown at 61 °C, decreasing by 0.6 °C per cycle for 60 s), followed by 29 additional cycles (94 °C for 20 s; 55 °C for 60 s). The plates were then read at 30 °C for endpoint fluorescent measurement.

Tracing lineage-specific *Ae. tauschii* haplotype blocks in the bread wheat genome

Missing link finder pipeline. We generated canonical 51-mers for each of the 82,293 genotyped wheat accessions from Sansaloni et al.[35] using their respective DArTseq markers and Jellyfish (v 2.3.0)[95]. For each accession, the *k*-mers were sorted and stored as text files. From the *k*-mer matrix available from Gaurav et al.[14], *k*-mers present only in *Ae. tauschii* L3 were extracted, sorted, and stored as text files. Pairwise comparisons of the sample-specific *k*-mers from the 82,293 wheat accessions and the L3-specific *k*-mers were performed using the comm bash command. Jaccard indices were computed with the following formula, where *A* is the set of *k*-mers from a single accession and *L* is the L3-specific *k*-mer set.

$$J(A, L) = \frac{A \cap L}{A \cup L}$$

The script is available on Github (https://github.com/emilecg/wheat_evolution).

Determining the extent of L3 in wheat lines using whole-genome re-sequencing data of 59 hexaploid wheat landraces. Raw reads were trimmed using Trimmomatic (v0.38)[61] with the following settings "ILLUMINACLIP:adapters.fa:2:30:10 LEADING:3 TRAILING:3 SLIDINGWINDOW:4:15 MINLEN:36". KMC (v3.1.2)[96] was used to generate 31-mer sets for the 59 resequenced wheat landraces (Supplementary Table 14). IBSpy (v0.4.6)[13] was run with TA2576 as a reference and the bread wheat landraces as queries with a *k*-mer size of 31 and a window size of 50,000 bp as parameters. A variation score threshold of ≤150 was used to determine how many windows were in common between the L3 reference and the wheat landraces. IBSpy variation values of ≤150 were determined to be optimal to account for the relatively low intra-lineage variation present in L3 (Extended Data Fig. 9 and Supplementary Table 32). The percentage of matching 50-kb windows was used as a proxy to determine the extent of introgression in the landraces.

Differences in genes in the 135-Mb L3 introgression block on chromosome 1D. The protein sequences of genes annotated in the interval of the introgression on the Kariega genome and on the CWI 86942 genome were compared using DIAMOND and visualized with the Persephone genome browser. In case genes were annotated in both the genomes, their amino acid sequences were aligned using the Needleman–Wunsch algorithm to determine the percentage of identity. The absence of genes in one of the two annotations was investigated manually with the BLAST algorithm integrated into Persephone. Annotated genes found to be part of transposable elements were excluded from the analysis.

Presence of the 135-Mb L3 haplotype block on chromosome 1D in wheat landraces. The presence of the 135-Mb L3 haplotype block was manually confirmed in 12 out of the 126 wheat landraces (Supplementary Table 16). CWI 86942 and another Georgian landrace (CWI 86929) had the largest block size (Extended Data Fig. 6d).

To further determine how widespread the presence of the chromosome 1D L3 segment was, we downloaded the IBSpy variation file from 1,035 hexaploid wheat accessions (827 landraces and 208 modern cultivars) and L3 line BW_01028 (https://opendata.earlham.ac.uk/wheat/under_license/toronto/WatSeq_2023-09-15_landrace_modern_Variation_Data/IBSpy_variations_10WheatGenomes/) against the Chinese Spring RefSeq v1.0 assembly[38]. We found an additional 20 wheat accessions that carry at least parts of this segment. We defined the start and end of the L3 segments in these 20 accessions by determining the difference between the variation value of BW_01028 (L3) and the corresponding variation value of the twenty accessions. If the difference was ≤150, we defined the accession to carry the L3 segment.

Bread wheat D genome subpopulations contribution

The approach used for a quantitative estimation of the contributions of the different subpopulations to the D genomes and the estimation of technical artifacts are described in Supplementary Note 3 and Supplementary Table 33. The manual curation process that allowed counting the minimal number of hybridizations required to explain the presence of different haplotypes is described in Supplementary Note 4.

Data visualization

We used the R package karyoploteR (v1.20.3)[97] for the haplotype representation of the chromosomes in Figs. 3d,e and 4b and Extended Data Fig. 7. The remaining plots were produced with ggplot2 (v3.4.2)[98] and the Python seaborn library (v0.11.2)[78]. Maps in Figs. 1a, 3c and 4a and Extended Data Fig. 6b were generated using QGIS (v3.32.3).

Germplasm availability

All the 60 wheat landraces analysed in this study listed in Supplementary Table 14 are available upon request from the CIMMYT (https://www.cimmyt.org/) and ICARDA (https://www.icarda.org/) gene banks. Seed of accessions from the Open Wild Wheat Consortium *Ae. tauschii* Diversity Panel collection, Cereal Crop Wild Relatives (*Triticeae*) collection, DFW Wheat Academic Toolkit collection and Deposited Published Research Material collection can be obtained from the Germplasm Resource Unit (GRU) of the John Innes Center; seed from accessions with WGRC bank ID as the only primary ID (Supplementary Table 1) can be obtained from the Wheat Genetics Resource Center (WGRC) of Kansas State University; 34 accessions can be obtained from the Plant Gene Resources of Canada (PGRC); 84 accessions donated by the Institute of Botany, Plant Physiology and Genetics of the Tajikistan National Academy of Sciences were deposited in the Wheat Genetics Resource Center (WGRC) as were 37 accessions donated by Quaid-i-Azam University; 20 accessions donated by the Azerbaijan National Academy of Sciences can be made available upon request.

Reporting summary

Further information on research design is available in the Nature Portfolio Reporting Summary linked to this article.

Data availability

The sequencing data and genome assemblies generated in this study were submitted to NCBI under BioProject number PRJNA956839, including the raw Illumina reads for 350 *Ae. tauschii* accessions, the raw PacBio reads, the Hi-C data, the raw RNA-seq reads from 5 tissues of *Ae. tauschii* accessions TA10171, TA1675 and TA2576, the raw Illumina reads for 59 wheat landraces and the raw PacBio reads and Omni-C data of the wheat landrace CWI 86942. The genome assemblies of the 46 *Ae. tauschii* accessions, the assemblies and annotations for CWI 86942, TA10171, TA1675 and TA2576, the variant call (SNP) file, the *k*-mer matrix for 920 *Ae. tauschii* accessions, the phylogenetic tree for 493 non-redundant *Ae. tauschii* accessions, the structural variant call (SV) files, the IBSpy variation tables, the predictions of the subpopulations contributing to the 17 hexaploid wheat assemblies, an excel file containing the RagTag scaffold output agp files and the dot-plots produced by MashMap used to validate the RagTag scaffolding are available at Dryad (https://doi.org/10.5061/dryad.vmcvdnd0d (ref. 99); https://doi.org/10.5061/dryad.wm37pvmvd (ref. 100); https://doi.org/10.5061/dryad.wpzgmsbvm (ref. 101); https://doi.org/10.5061/dryad.p5hqbzkvx (ref. 102)). The *Lr39* genomic sequence was deposited in NCBI Genbank under accession number OR567850. The TA10171 (L1), TA1675 (L2) and TA2576 (L3) genomes are available for online BLAST, Jbrowse visualization and synteny analysis with the currently available *Triticinae* genomes at (https://wheat.pw.usda.gov/GG3pangenome/wheat/D/taus_home.php). The Ensembl nrTEplants repetitive element database (June 2020) was used for repeat content prediction. *Viridiplantae* protein models from OrthoDB v.11 were used to predict de novo gene models for the annotated *Ae. tauschii* genomes. The predicted translated proteins were annotated using the following databases: FunFam, SFLD, PANTHER, Gene3D, PRINTS, Coils, SUPERFAMILY, SMART, CDD, PIRSR, ProSitePatterns, AntiFam, Pfam, MobiDBLite, PIRSF and NCBIfam. We downloaded sequencing data for 306 accessions from NCBI BioProject number PRJNA685125, 275 accessions from NCBI BioProject number PRJNA705859, and 24 accessions from the China National Center for Bioinformation–National Genomics Data Center under accession number PRJCA005979.

Code availability

The *k*-mer matrix generation pipeline for large diversity panels is available at GitHub (https://github.com/githubcbrc/KGWASMatrix). The custom script for estimating the cumulative *k*-mer content is available at GitHub (https://github.com/andreagonzam/tauschii_pangenome). The custom scripts for Missing Link Finder pipeline and haplotype analysis are available at GitHub (https://github.com/emilecg/wheat_evolution).

47. Abrouk, M. et al. Fonio millet genome unlocks African orphan crop diversity for agriculture in a changing climate. *Nat. Commun.* **11**, 4488 (2020).
48. Thachuk, C. et al. Core Hunter: an algorithm for sampling genetic resources based on multiple genetic measures. *BMC Bioinformatics* **10**, 243 (2009).
49. Driguez, P. et al. LeafGo: Leaf to Genome, a quick workflow to produce high-quality de novo plant genomes using long-read sequencing technology. *Genome Biol.* **22**, 256 (2021).
50. Cheng, H. Y., Concepcion, G. T., Feng, X. W., Zhang, H. W. & Li, H. Haplotype-resolved de novo assembly using phased assembly graphs with hifiasm. *Nat. Methods* **18**, 170–175 (2021).
51. Gurevich, A., Saveliev, V., Vyahhi, N. & Tesler, G. QUAST: quality assessment tool for genome assemblies. *Bioinformatics* **29**, 1072–1075 (2013).
52. Rhie, A., Walenz, B. P., Koren, S. & Phillippy, A. M. Merqury: reference-free quality, completeness, and phasing assessment for genome assemblies. *Genome Biol.* **21**, 245 (2020).
53. Bankevich, A., Bzikadze, A. V., Kolmogorov, M., Antipov, D. & Pevzner, P. A. Multiplex de Bruijn graphs enable genome assembly from long, high-fidelity reads. *Nat. Biotechnol.* **40**, 1075–1081 (2022).
54. Padmarasu, S., Himmelbach, A., Mascher, M. & Stein, N. in *Plant Long Non-Coding RNAs: Methods and Protocols*, Vol. 1933 (eds Chekanova, J. A. & Wang, H.-L. V.) 441–472 (Springer, 2019).
55. Himmelbach, A., Walde, I., Mascher, M. & Stein, N. Tethered chromosome conformation capture sequencing in *Triticeae*: a valuable tool for genome assembly. *Bio Protoc.* **8**, e2955 (2018).
56. Durand, N. C. et al. Juicer provides a one-click system for analyzing loop-resolution Hi-C experiments. *Cell Syst.* **3**, 95–98 (2016).
57. Dudchenko, O. et al. De novo assembly of the *Aedes aegypti* genome using Hi-C yields chromosome-length scaffolds. *Science* **356**, 92–95 (2017).
58. Durand, N. C. et al. Juicebox provides a visualization system for Hi-C contact maps with unlimited zoom. *Cell Syst.* **3**, 99–101 (2016).
59. Alonge, M. et al. Automated assembly scaffolding using RagTag elevates a new tomato system for high-throughput genome editing. *Genome Biol.* **23**, 258 (2022).
60. Jain, C., Koren, S., Dilthey, A., Phillippy, A. M. & Aluru, S. A fast adaptive algorithm for computing whole-genome homology maps. *Bioinformatics* **34**, i748–i756 (2018).
61. Bolger, A. M., Lohse, M. & Usadel, B. Trimmomatic: a flexible trimmer for Illumina sequence data. *Bioinformatics* **30**, 2114–2120 (2014).
62. Dobin, A. et al. STAR: ultrafast universal RNA-seq aligner. *Bioinformatics* **29**, 15–21 (2013).
63. Danecek, P. et al. Twelve years of SAMtools and BCFtools. *Gigascience* **10**, giab008 (2021).
64. Brůna, T., Hoff, K. J., Lomsadze, A., Stanke, M. & Borodovsky, M. BRAKER2: automatic eukaryotic genome annotation with GeneMark-EP+ and AUGUSTUS supported by a protein database. *NAR Genom. Bioinformatics* **3**, lqaa108 (2021).
65. Hoff, K. J., Lange, S., Lomsadze, A., Borodovsky, M. & Stanke, M. BRAKER1: unsupervised RNA-Seq-based genome annotation with GeneMark-ET and AUGUSTUS. *Bioinformatics* **32**, 767–769 (2016).
66. Hoff, K. J., Lomsadze, A., Borodovsky, M. & Stanke, M. in *Gene Prediction: Methods and Protocols*, Vol. 1962 (ed. Kollmar, M.) 65–95 (Springer, 2019).
67. Camacho, C. et al. BLAST+: architecture and applications. *BMC Bioinformatics* **10**, 421 (2009).
68. Blum, M. et al. The InterPro protein families and domains database: 20 years on. *Nucleic Acids Res.* **49**, D344–D354 (2021).
69. Jones, P. et al. InterProScan 5: genome-scale protein function classification. *Bioinformatics* **30**, 1236–1240 (2014).
70. Emms, D. M. & Kelly, S. OrthoFinder: phylogenetic orthology inference for comparative genomics. *Genome Biol.* **20**, 238 (2019).
71. Smit, A., Hubley, R. & Green, P. RepeatMasker Open-4.0 http://www.repeatmasker.org (2015).
72. Contreras-Moreira, B. et al. K-mer counting and curated libraries drive efficient annotation of repeats in plant genomes. *Plant Genome* **14**, e20143 (2021).
73. Abrouk, M. et al. Chromosome-scale assembly of the wild wheat relative *Aegilops umbellulata*. *Sci. Data* **10**, 739 (2023).
74. Shumate, A. & Salzberg, S. L. Liftoff: accurate mapping of gene annotations. *Bioinformatics* **37**, 1639–1643 (2021).
75. Pertea, G. & Pertea, M. GFF utilities: GffRead and GffCompare. *F1000Research* **9**, 304 (2020).
76. Buchfink, B., Reuter, K. & Drost, H.-G. Sensitive protein alignments at tree-of-life scale using DIAMOND. *Nat. Methods* **18**, 366–368 (2021).
77. Virtanen, P. et al. SciPy 1.0: fundamental algorithms for scientific computing in Python. *Nat. Methods* **17**, 261–272 (2020).
78. Waskom, M. L. Seaborn: statistical data visualization. *J. Op. Source Softw.* **6**, 3021 (2021).
79. Li, H. Aligning sequence reads, clone sequences and assembly contigs with BWA-MEM. Preprint at *arXiv* https://doi.org/10.48550/arXiv.1303.3997 (2013).
80. Cook, D. E. & Andersen, E. C. VCF-kit: assorted utilities for the variant call format. *Bioinformatics* **33**, 1581–1582 (2017).
81. Gain, C. & François, O. LEA 3: Factor models in population genetics and ecological genomics with R. *Mol. Ecol. Resour.* **21**, 2738–2748 (2021).
82. Danecek, P. et al. The variant call format and VCFtools. *Bioinformatics* **27**, 2156–2158 (2011).
83. Wei, F., Wing, R. A. & Wise, R. P. Genome dynamics and evolution of the *Mla* (powdery mildew) resistance locus in barley. *Plant Cell* **14**, 1903–1917 (2002).
84. Stecher, G., Tamura, K. & Kumar, S. Molecular Evolutionary Genetics Analysis (MEGA) for macOS. *Mol. Biol. Evol.* **37**, 1237–1239 (2020).
85. Tamura, K., Stecher, G. & Kumar, S. MEGA11: Molecular Evolutionary Genetics Analysis version 11. *Mol. Biol. Evol.* **38**, 3022–3027 (2021).
86. Kolmer, J., Bajgain, P., Rouse, M., Li, J. & Zhang, P. Mapping and characterization of the recessive leaf rust resistance gene *Lr83* on wheat chromosome arm 1DS. *Theor. Appl. Genet.* **136**, 115 (2023).
87. Long, D. & Kolmer, J. A North American system of nomenclature for *Puccinia recondita* f. sp. *tritici*. *Phytopathology* **79**, 525–529 (1989).
88. Wang, S. et al. Characterization of polyploid wheat genomic diversity using a high-density 90,000 single nucleotide polymorphism array. *Plant Biotechnol. J.* **12**, 787–796 (2014).
89. Pestsova, E., Ganal, M. & Röder, M. Isolation and mapping of microsatellite markers specific for the D genome of bread wheat. *Genome* **43**, 689–697 (2000).
90. Heffelfinger, C., Fragoso, C. A. & Lorieux, M. Constructing linkage maps in the genomics era with MapDisto 2.0. *Bioinformatics* **33**, 2224–2225 (2017).
91. Voorrips, R. E. MapChart: software for the graphical presentation of linkage maps and QTLs. *J. Heredity* **93**, 77–78 (2002).
92. Lück, S. et al. siRNA-Finder (si-Fi) software for RNAi-target design and off-target prediction. *Front. Plant Sci.* **10**, 1023 (2019).
93. Barnes, C. W. & Szabo, L. J. Detection and identification of four common rust pathogens of cereals and grasses using real-time polymerase chain reaction. *Phytopathology* **97**, 717–727 (2007).
94. Chang, Q. et al. A unique invertase is important for sugar absorption of an obligate biotrophic pathogen during infection. *New Phytol.* **215**, 1548–1561 (2017).
95. Marçais, G. & Kingsford, C. A fast, lock-free approach for efficient parallel counting of occurrences of *k*-mers. *Bioinformatics* **27**, 764–770 (2011).
96. Kokot, M., Długosz, M. & Deorowicz, S. KMC 3: counting and manipulating *k*-mer statistics. *Bioinformatics* **33**, 2759–2761 (2017).
97. Gel, B. & Serra, E. karyoploteR: an R/Bioconductor package to plot customizable genomes displaying arbitrary data. *Bioinformatics* **33**, 3088–3090 (2017).
98. Wickham, H. *ggplot2: Elegant Graphics for Data Analysis* (Springer-Verlag, 2016).
99. Cavalet-Giorsa, E. et al. Population genomics of the wild wheat *Aegilops tauschii* (Open wild wheat consortium phase II) [Dataset]. *Dryad* https://doi.org/10.5061/dryad.vmcvdnd0d (2024).
100. Cavalet-Giorsa, E. et al. *k*-mer matrix *Aegilops tauschii* diversity panel (Open wild wheat consortium phase II) Part 3/3 [Dataset]. *Dryad* https://doi.org/10.5061/dryad.wm37pvmvd (2024).
101. Cavalet-Giorsa, E. et al. *k*-mer matrix *Aegilops tauschii* diversity panel (Open wild wheat consortium phase II) Part 2/3 [Dataset]. *Dryad* https://doi.org/10.5061/dryad.wpzgmsbvm (2024).
102. Cavalet-Giorsa, E. et al. *k*-mer matrix *Aegilops tauschii* diversity panel (Open wild wheat consortium phase II) Part 1/3 [Dataset]. *Dryad* https://doi.org/10.5061/dryad.p5hqbzkvx (2024).

Acknowledgements This research used the Shaheen supercomputer and the Ibex cluster managed by the Supercomputing Core Laboratory at King Abdullah University of Science and Technology (KAUST). We thank the systems administrators and computational scientists for help with debugging and overall support. The authors thank B. Steuernagel, D. Keyes, L. Fabbian and K. G. Kise for bioinformatics advice; E. P. Faig for greenhouse assistance; I. Walde for technical assistance with Hi-C library preparation and sequencing; H. Guo for administering the OWWC sequencing; J. Poland and L. Gao for advice on PacBio sequencing; A. Bentley, B. Keller, H. Bürstmayr, J. Faris, M. Maccaferri, M. Bozzoli, R. Horsnell, D. Seung, J. Balk, R. McNelly and T. O'Hara for nominating *Ae. tauschii* lines of strategic interest; R. McIntosh for critical reading of the manuscript; E. Waller for assistance with the OWWC website; GrainGenes resources for hosting the online database; USDA for infrastructure support in terms of providing computational resources at SCINet high performance cluster; and University of Maryland supercomputing resources (http://hpcc.umd.edu) for computational work for the database. This publication is based on work supported by KAUST awards ORFS-CRG10-2021-4735 to B.B.H.W., ORFS-CRG11-2022-5076 to S.G.K. and URF/1/4352-01-01, FCC/1/1976-44-01, FCC/1/1976-45-01, REI/1/5234-01-01 and REI/1/5414-01-01 to X.G.; Australian Government Research Training Program and the University of Queensland Centennial Scholarships to N.A. during genetic mapping of *Lr39*; Academy of Scientific Research and Technology (ASRT) project ID 19385 and Climate Change Adaptation and Nature Conservation (GREEN FUND-ASRT) to A.F.E.; National Major Agricultural Science and Technology project NK2022060101 and National Key Research and Development Program of China 2021YFF1000204 to L.M.; a Genebank3.0 project from the German Federal Ministry of Education and Research (grant no. FKZ 031B1300A) to J.C.R.; grants from the Next-Generation BioGreen 21 Linked Program (PJ015786) of the Rural Development Administration (RDA), South Korea to J.-Y.L.; RDA/USDA-ARS cooperation agreement no. 58-0210-9-226-F to J.-Y.L. and Y.Q.G.; ARS project 2030-21430-015-000 to S.S.X. and Y.Q.G.; the UK Biotechnology and Biological Sciences Research Council (BBSRC) Institute Strategic Programme Designing Future Wheat (BB/P016855/1) and a European Research Council grant (ERC-2019-COG-866328) to C.U.; the Mexican Consejo Nacional de Ciencia y Tecnología (CONACYT; 2018-000009-01EXTF-00306) to J.Q.-C.; funding from Department of Biotechnology, Government of India to P.C. and S.K.; USDA-NIFA Capacity Fund via South Dakota Agricultural Experiment Station to W.L.; a Bayer (previously Monsanto) Beachell Borlaug International Scholar's Program to S. Ghosh; National Science Foundation of United States grant number 2102953 to J.D.; ARS Project 2030-21000-056-00D to G.R.L.; an USDA-NIFA Grant (2022-67013-36362) to V.K.T.; a NERC Independent Research Fellowship (NE/T011025/1) to L.T.D.; and 4D Wheat: Diversity, Domestication, Discovery and Delivery project (C.J.P.), funded by Genome Canada, Agriculture and Agri-Food Canada, Western Grains Research Foundation, Saskatchewan Ministry of Agriculture, Saskatchewan Wheat Development Commission, Alberta Wheat Commission, Manitoba Crop Alliance, Ontario Research Fund, and the Canadian Agricultural Partnership.

Author contributions A.G.-M., C.G., E.C.-G., S.M.R., A.R., N.C., A.B.P., C.-Y.H., K.D.L., W.J.R., F.Y.N., S. Grewal, G.S.B. and B.B.H.W. configured *Ae. tauschii* diversity panel and distributed seed. A.G.-M., A.P., A.B.P. and C.-Y.H. extracted *Ae. tauschii* DNA. S.H., M. Abbasi, M.L., N.K. and G.S.B. sampled tissue and extracted RNA from *Ae. tauschii*. A.G.-M., S.H., A.F.E., L.M., A. Sharon, A.H., J.C.R., M.K., M.M., N.S., D.P., S.L., J.-Y.L., P.C., S.K., P.Z., R.F.P., D.-C.L., W.L., J.D., V.K.T., S. Grewal, C.J.P., H.S.C., J.E., L.T.D., S.S.X., Y.Q.G., X.X., G.S.B. and B.B.H.W. outlined *Ae. tauschii* sequencing strategy and acquired DNA and RNA sequences. E.C.-G. and N.A. extracted DNA for bread wheat landraces. A.G.-M., E.C.-G., S.H., L.F.R., H.S.C. and M. Abrouk undertook sequence data quality control, curation, back-up and/or distribution. A. Salhi, X.G. and S.B. assembled *k*-mer matrix. E.C.-G. performed variant calling and filtering. A.G.-M. and E.C.-G. performed redundancy analysis. E.C.-G. and A.G.-M. performed genome-wide phylogenetic analysis and E.C.-G. performed structure analysis. A.G.-M. and H.S.C. assembled *Ae. tauschii* genomes and A.G.-M. assessed their quality. S.H. and M. Abrouk performed genome annotations. A.G.-M. performed structural variant analysis. A.G.-M. performed *k*-mer GWAS. N.A., M.P., S. Ghosh, R.C., Y.W., E.L.O., P.Z., R.F.P., W.B.M., W.H.P.B., B.J.S., J.A.K. and O.M. performed rust phenotyping. A.G.-M. and E.C.-G. performed *Sr33* and *Sr66* comparative genomics analyses. N.A., E.S.L., Y.D. and S.K.P. generated bi-parental population and mapped *Lr39*. N.A. and Y.W. identified *Lr39* candidate gene, performed VIGS and annotated *Lr39*. E.C.-G. developed the 'Missing Link Finder' pipeline, identified L3-enriched bread wheat lines, and assembled CWI 86942 genome. C.U. and J.Q.-C. provided prepublication access to and helped implement IBSpy pipeline, and E.C.-G., C.U. and J.Q.-C. identified L3 haploblocks in wheat and calculated their accumulative size. E.C.-G. assigned extant wheat genome segments to ancestral *Ae. tauschii* populations and determined the minimum number of hybridizations. G.Y. and H.I.A. provided scientific advice. P.K.S., G.R.L. and V.K.T. implemented the *Ae. tauschii* genome database. E.C.-G., A.G.-M., N.A., S.H., A. Salhi, M. Abrouk, S.B., G.S.B., B.B.H.W. and S.G.K. conceived and designed experiments. E.C.-G., A.G.-M., N.A., C.G., B.B.H.W. and S.G.K. designed figures. S.G.K., E.C.-G., A.G.-M. and B.B.H.W. drafted first version of the manuscript with inputs and edits from N.A., S.H., A. Salhi, C.G., G.S.B. and S. Ghosh. A.G.-M. and B.B.H.W. managed the Open Wild Wheat Consortium (www.openwildwheat.org). All authors read, commented on and approved the final version of the manuscript. Authors are grouped by institution acronym and then by first name in the author list and author contribution statement, except for the first seven and last six authors in the list.

Competing interests The authors declare no competing interests.

Additional information

Supplementary information The online version contains supplementary material available at https://doi.org/10.1038/s41586-024-07808-z.

Correspondence and requests for materials should be addressed to Brande B. H. Wulff or Simon G. Krattinger.

Peer review information *Nature* thanks Anthony Hall, John Lovell and the other, anonymous, reviewer(s) for their contribution to the peer review of this work. Peer review reports are available.

Reprints and permissions information is available at http://www.nature.com/reprints.

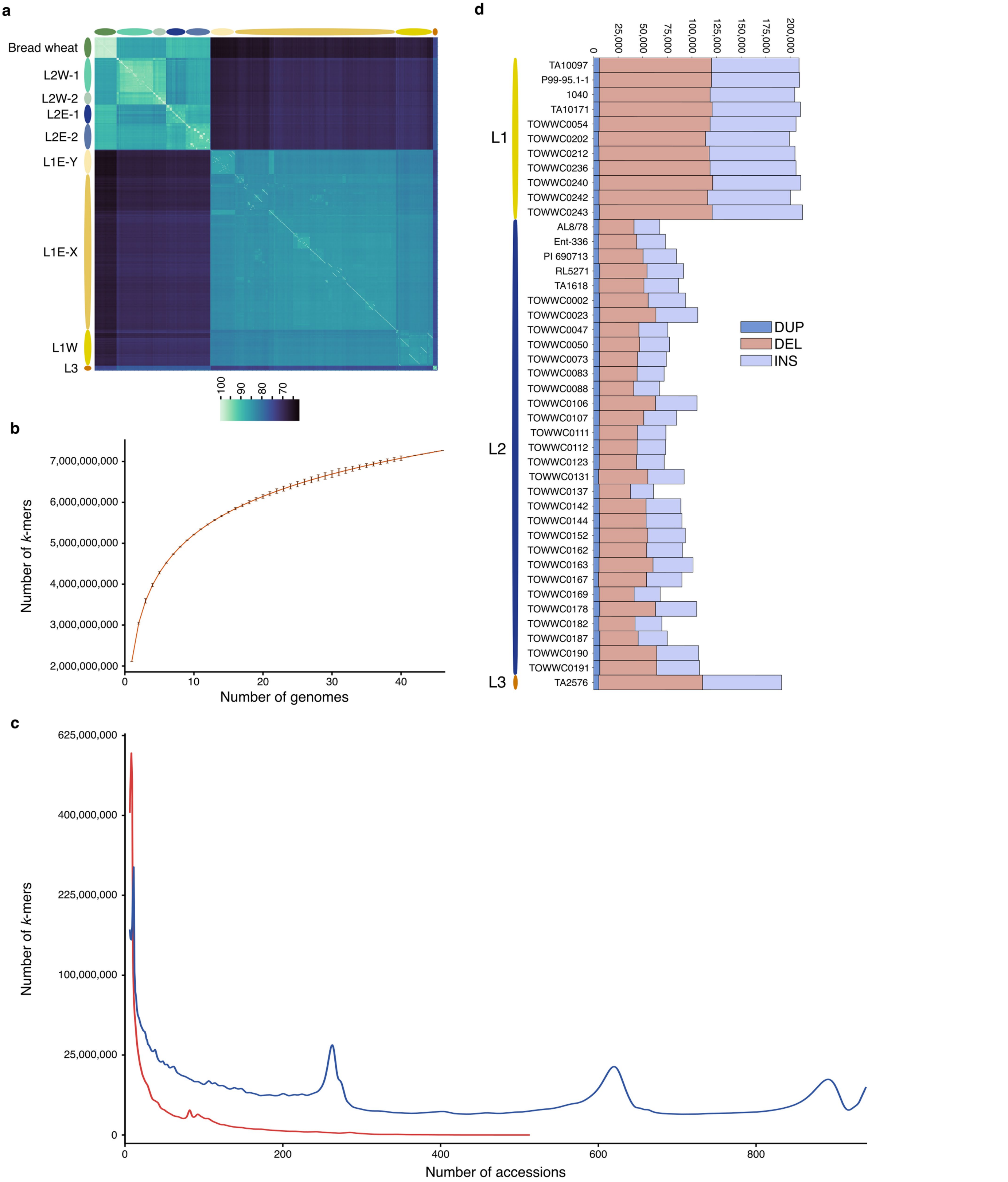

Extended Data Fig. 1 | *Aegilops tauschii* genomic resources. a, Clustered heatmap showing SNP-based pairwise identity across 957 *Ae. tauschii* accessions and 59 bread wheat landraces. The different *Ae. tauschii* subpopulations are indicated on the left. **b**, Logarithmic curve fit to *k*-mer accumulation across the 46 *Ae. tauschii* accessions selected for high-quality genome assemblies. The vertical bars show the standard deviation. **c**, *k*-mer frequency distributions across 920 *Ae. tauschii* accessions. The red curve shows *k*-mers that are absent in the 46 accessions selected for high-quality genome assemblies. The blue curve shows *k*-mers present in the 46 accessions. The peaks at ~250 and ~600 correspond to L2 and L1-specific *k*-mers, respectively. A square root function was applied to the y-axis for better visualization. **d**, Number of structural variants across *Ae. tauschii* accessions from lineages 1, 2 and 3 relative to the chromosome-scale assembly of L2 accession TA1675. Shown are duplications (DUP), deletions (DEL), and insertions (INS) ranging from 50 bp to 100 kb.

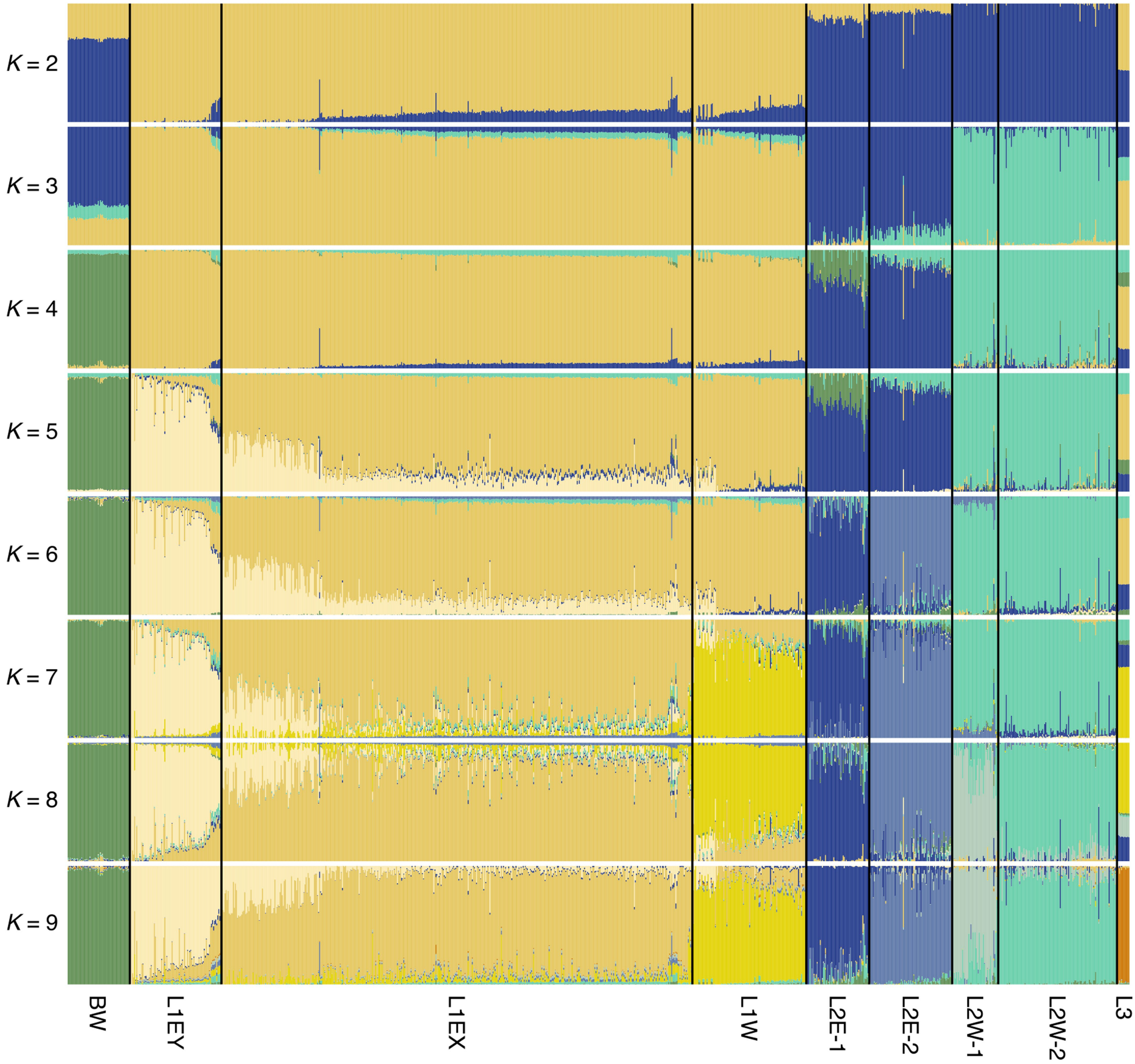

Extended Data Fig. 2 | *Ae. tauschii* population structure from *K* = 2 to *K* = 9. Each vertical bar represents an accession and the bars are filled by colours representing the proportion of each ancestry. The subpopulation designations are described in the main text. BW = bread wheat.

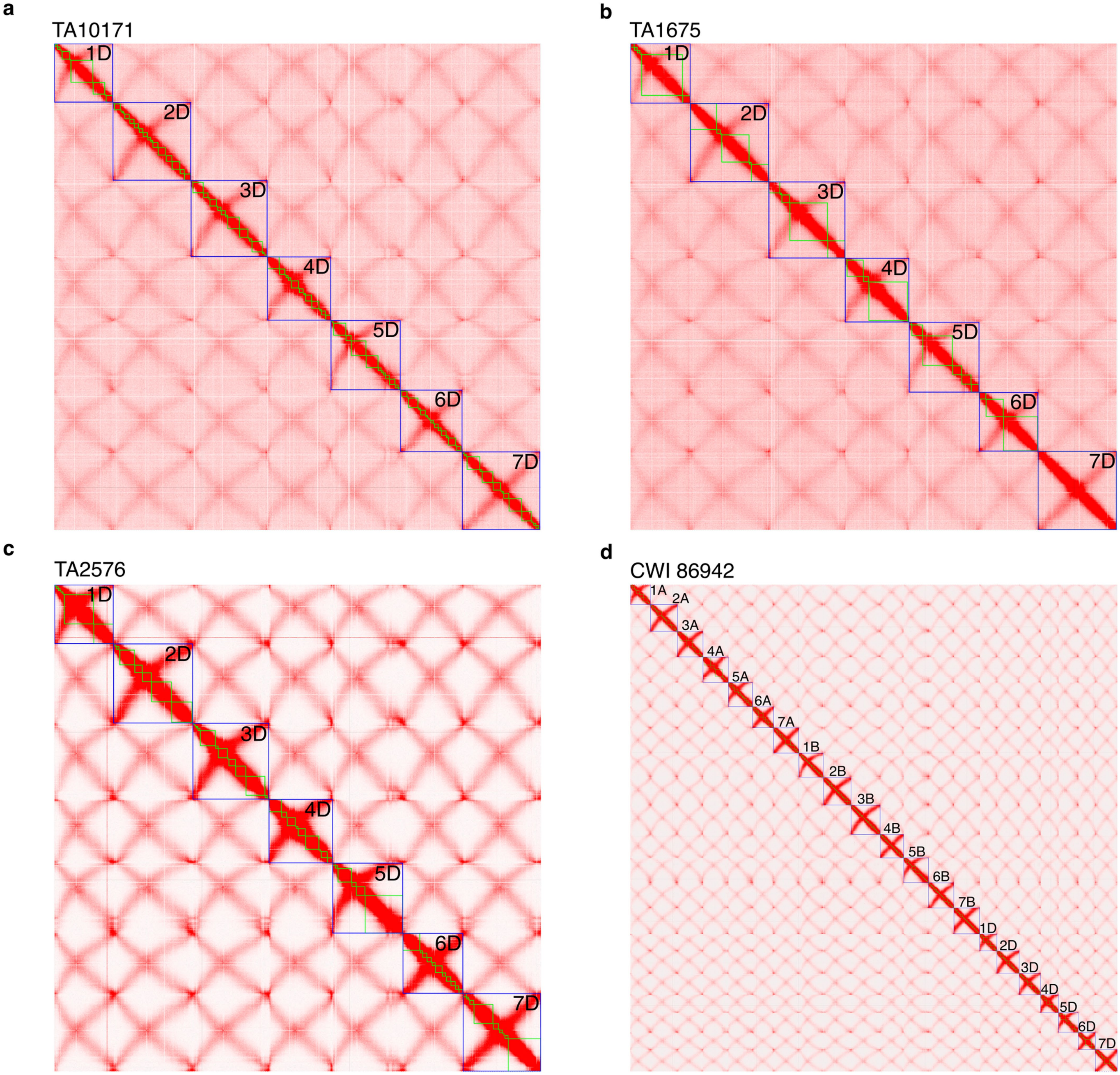

Extended Data Fig. 3 | Chromosome contact maps of *Ae. tauschii* accessions TA10171 (a), TA1675 (b), TA2576 (c), and bread wheat accession CWI 86942 (d). Green boxes represent individual PacBio contigs. Blue boxes indicate chromosomes. Chromosome 7D of TA1675 was assembled as a single PacBio contig.

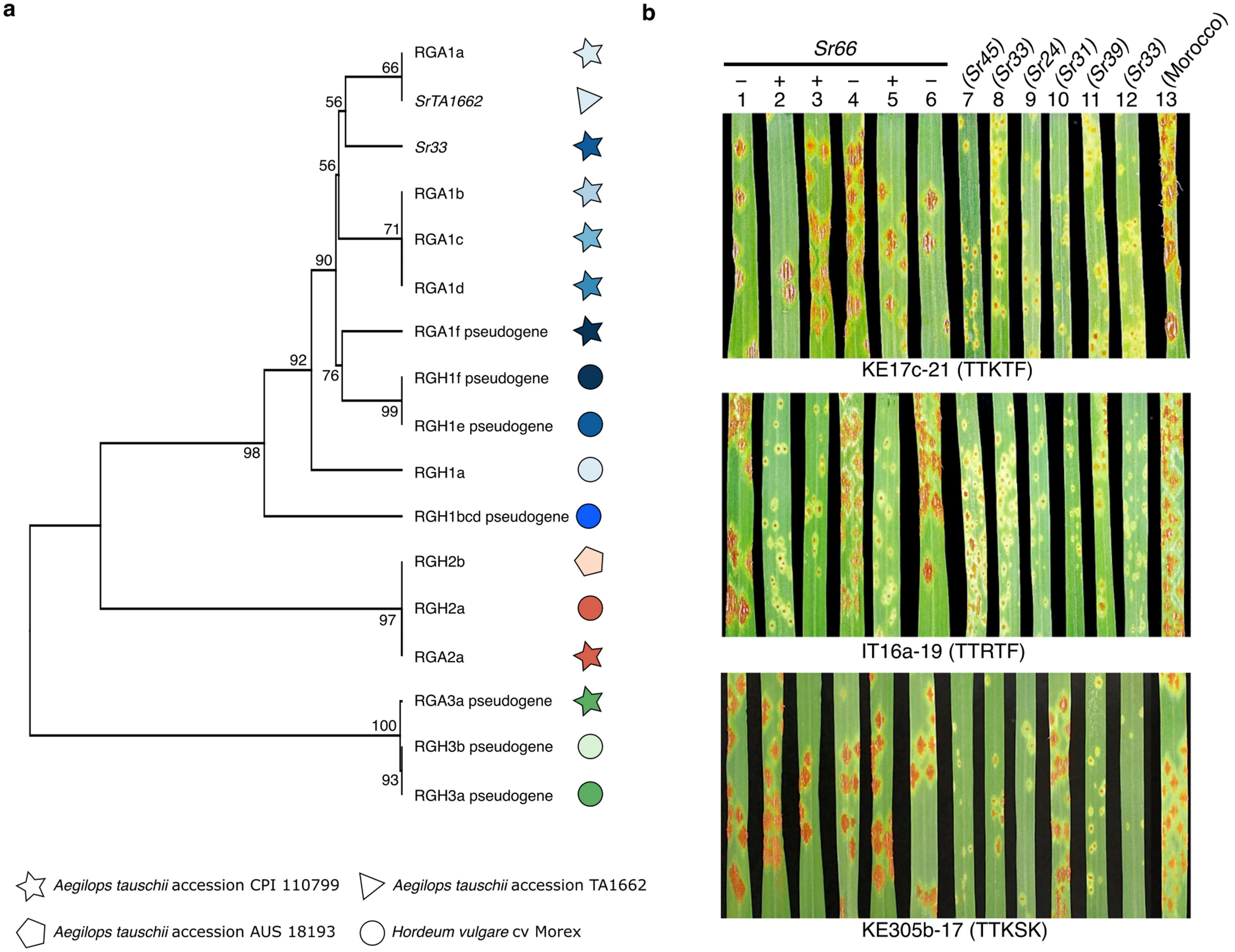

Extended Data Fig. 4 | Haplotype analysis leads to the designation of stem rust resistance gene *Sr66*. a, Phylogeny showing the relationship across *Mla* genes from *Ae. tauschii* and barley. Resistance Gene Analogs (RGA) represent *Ae. tauschii* and Resistance Gene Homologs (RGH) represent barley cultivar Morex. The *Ae. tauschii* RGA gene sequences were derived from different accessions (Supplementary Table 10). RGA/RGH families 1, 2 and 3 are indicated in blue, red and green, respectively. The tree was constructed using the unweighted UPGMA algorithm. Bootstrap support values are shown based on 5,000 replicates. **b**, *SrTA1662* (*Sr66*) and *Sr33* display different race specificities. Reactions to *Puccinia graminis* f. sp. *tritici* isolates KE17c-21 (race TTKTF), IT16a-19 (TTRTF), and KE305b-17 (TTKSK) of transgenic *SrTA1662* (*Sr66*) wheat lines and non-transgenic nulls (1 to 6) and wheat *Sr* gene introgression lines and controls (7 to 13). 1, Fielder null (DPRM0050); 2, *Sr66* (DPRM0051); 3, *Sr66* (DPRM0059); 4, Fielder null (DPRM0062); 5, *Sr66* (DPRM0071); 6, Fielder null (DPRM0072); 7. *Sr45* (RL5406); 8. *Sr33* (RL5405); 9. *Sr24* (LcSr24Ag); 10. *Sr31* (Little Club/Agent (CI 13523)); 11. *Sr39* (RL5711); 12. *Sr33* (Chinese Spring); 13. cv. Morocco.

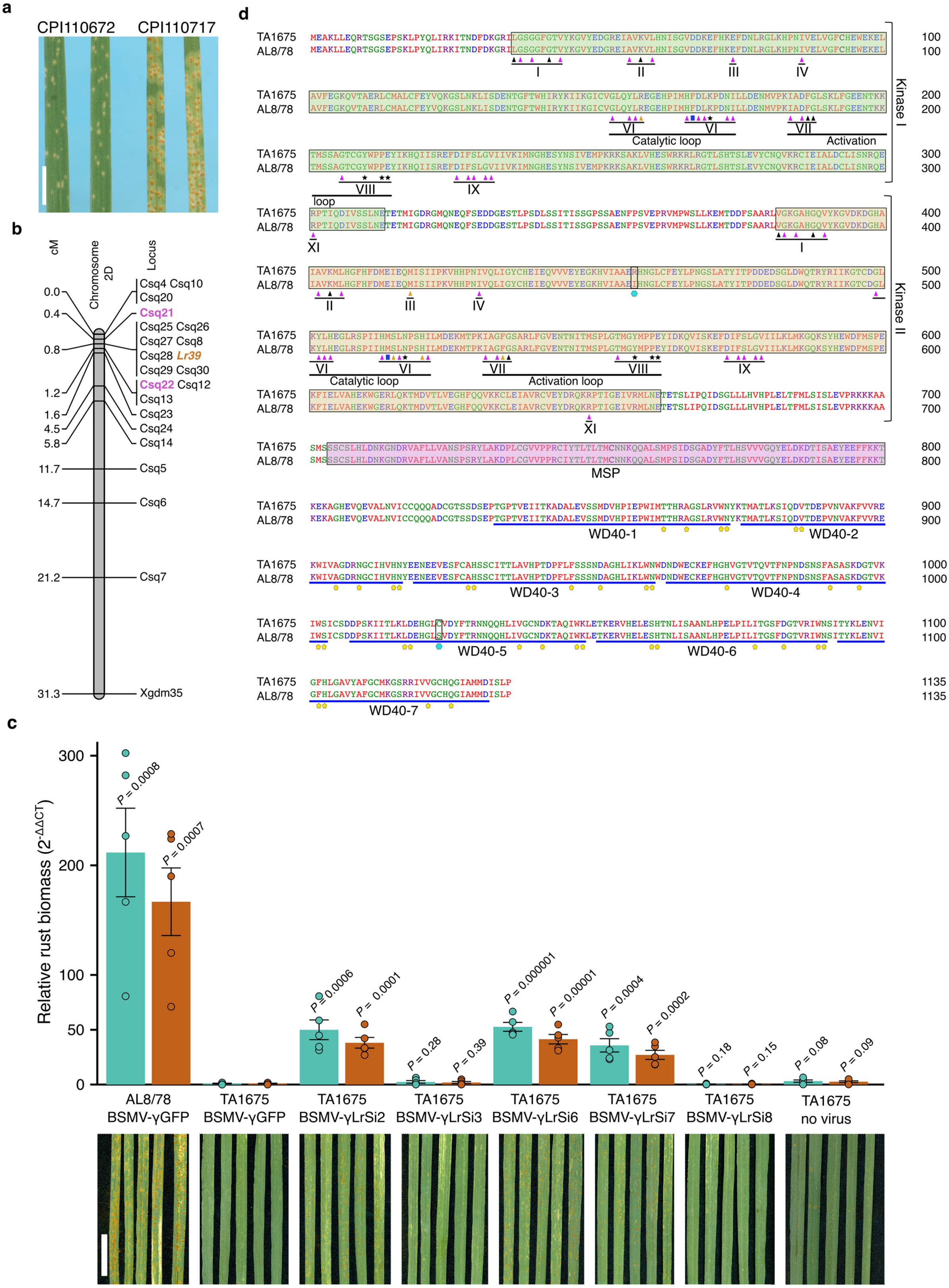

Extended Data Fig. 5 | See next page for caption.

Extended Data Fig. 5 | Bi-parental genetic mapping of *LR39* and analysis of key conserved domains in Lr39. a, Phenotypes of *Ae. tauschii* parents inoculated with the *Puccinia triticina* race Pt 26-1,3 (accession 316). CPI110672 (synonymous TA1675) carries *Lr39*. CPI110717 is the susceptible parent. Scale bar = 1 cm. **b**, Fine mapping of *LR39* in chromosome arm 2DS. Markers *Csq21* and *Csq22* are flanking the *LR39* locus whereas *Csq8*, *Csq25*, *Csq26*, *Csq27*, *Csq28*, *Csq29* and *Csq30* are co-segregating. **c**, Fungal biomass quantification using qPCR after virus-induced gene silencing (VIGS). Cereal rust specific primers amplifying the 28 S large subunit region (LSU - blue) or the internal transcribed spacer 1 (ITS1 - red) were used. Values represent means and error bars standard errors. Statistical analyses were done using a two tailed *t*-test against the TA1675 γGFP control. BSMV-γLrSi2, BSMV-γLrSi6, and BSMV-γLrSi7 are silencing constructs specific for the *WTK* gene. BSMV-γLrSi3 and BSMV-γLrSi8 are silencing construct specific for the *NLR* gene. N = 5 independent biological replicates. Scale bar = 5 cm. **d**, Analysis of key conserved domains of the Lr39 protein. The kinase 1 domain is highlighted by a green box, kinase 2 by a yellow box, the major sperm protein (MSP) domain by a pink box, and the seven WD40-repeats are underlined by blue lines. Roman numerals represent conserved kinase subdomains. Black triangles = ATP binding site predicted by InterPro; magenta triangles = key conserved residues; black asterisks = putative substrate binding site; blue squares = residue determining RD and non-RD kinases; brown triangles = polymorphism in the key conserved residues. In kinase 1, a key residue histidine is replaced by arginine in subdomain VI. In kinase 2, substitutions of residues glutamic acid to methionine in subdomain III, aspartic acid to serine and asparagine to histidine in subdomain VI form a catalytic loop, and aspartic acid to glycine in subdomain VII in the activation loop. Yellow pentagons = key conserved residues of WD40 repeats predicted by InterPro. Cyan hexagon = two polymorphic residues of TA1675 compared to AL8/78.

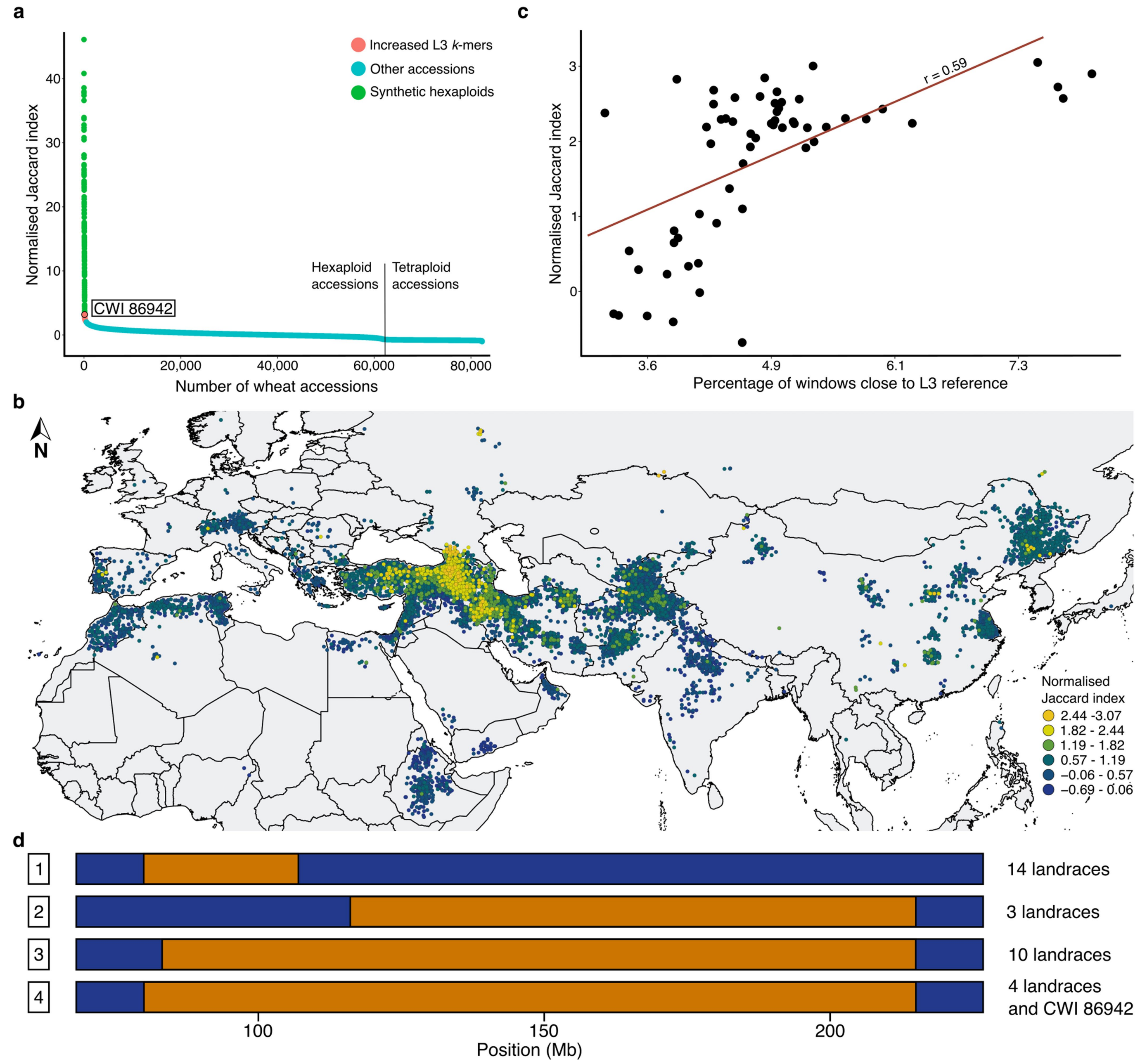

Extended Data Fig. 6 | Tracing lineage-specific *Ae. tauschii* haplotype blocks in bread wheat. **a**, Normalized Jaccard scores across 82,293 wheat accessions (including the 139 synthetic hexaploid wheats). Green indicates 139 synthetic hexaploid wheat accessions with *k*-mer enrichments of up to 40-fold. Red indicates bread wheat landraces with increased (2 to 3-fold) normalized Jaccard index. **b**, The Jaccard indices show a gradual decline with increasing geographic distance from Georgia. Dots represent individual bread wheat accessions for which exact coordinates were available. Colors represent different normalized Jaccard indices. **c**, Correlation between normalized Jaccard indices and the percentage of L3 genome based on whole-genome sequencing data. **d**, Diagram of a portion of chromosome arm 1DS. The chromosome positions indicated in Mb are according to the CWI 86942 assembly. Haplotype blocks corresponding to *Ae. tauschii* L2 are indicated in blue, and L3 in orange. Shown are different lengths of the L3 haplotype segment in various bread wheat lines. 1, CWI 84680, CWI 84694, CWI 84704, CWI 84686, CWI 14537, GEO-L1, WATDE0105, WATDE0944, WATDE0957, WATDE1005, WATDE1018, WATDE1017, WATDE0113, WATDE1010; 2, C33, WATDE1031, WATDE1032; 3, BW 50849, CWI 14244, CWI 28055, WATDE0026, WATDE0749, WATDE0047, WATDE0739, WATDE0999, WATDE1003, WATDE0993; 4, CWI 86929, CWI 86942, WATDE0975, WATDE0973, WATDE0974. The IBSpy variation values for the Watkins lines (WATDE) were extracted from Cheng et al.[38].

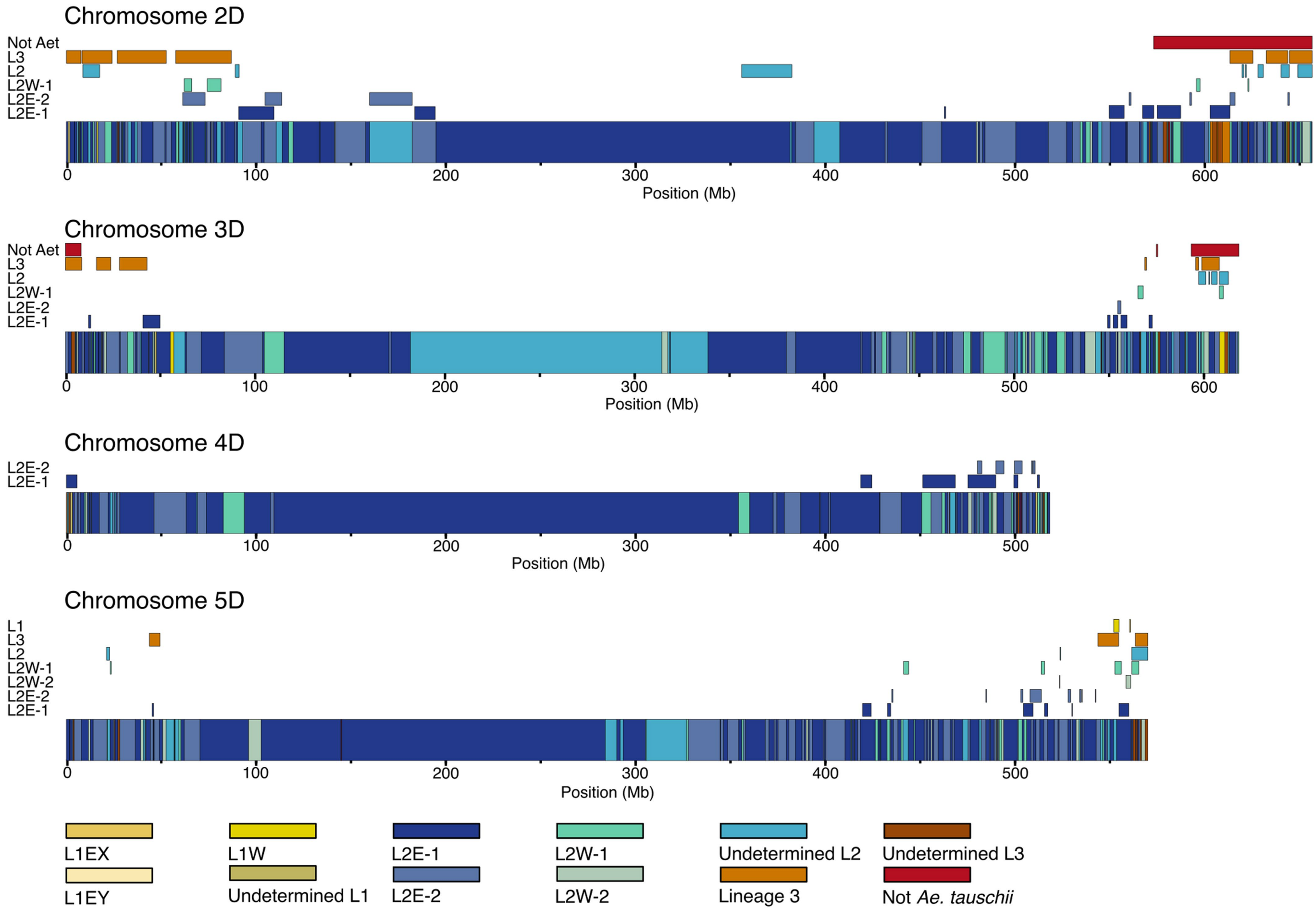

Extended Data Fig. 7 | Minimal number of hybridizations that gave rise to the extant bread wheat D genome. Shown are graphical representations of Chinese Spring chromosomes 2D, 3D, 4D and 5D. The colored boxes in the chromosomes represent the haplotypes found in Chinese Spring. Colored rectangles above the chromosomes represent alternative haplotype blocks identified across 126 hexaploid wheat landraces (cumulative length of alternative haplotype blocks across all 126 landraces). Colors refer to the *Ae. tauschii* subpopulations following the legend. The maximum number of haplotype blocks is four.

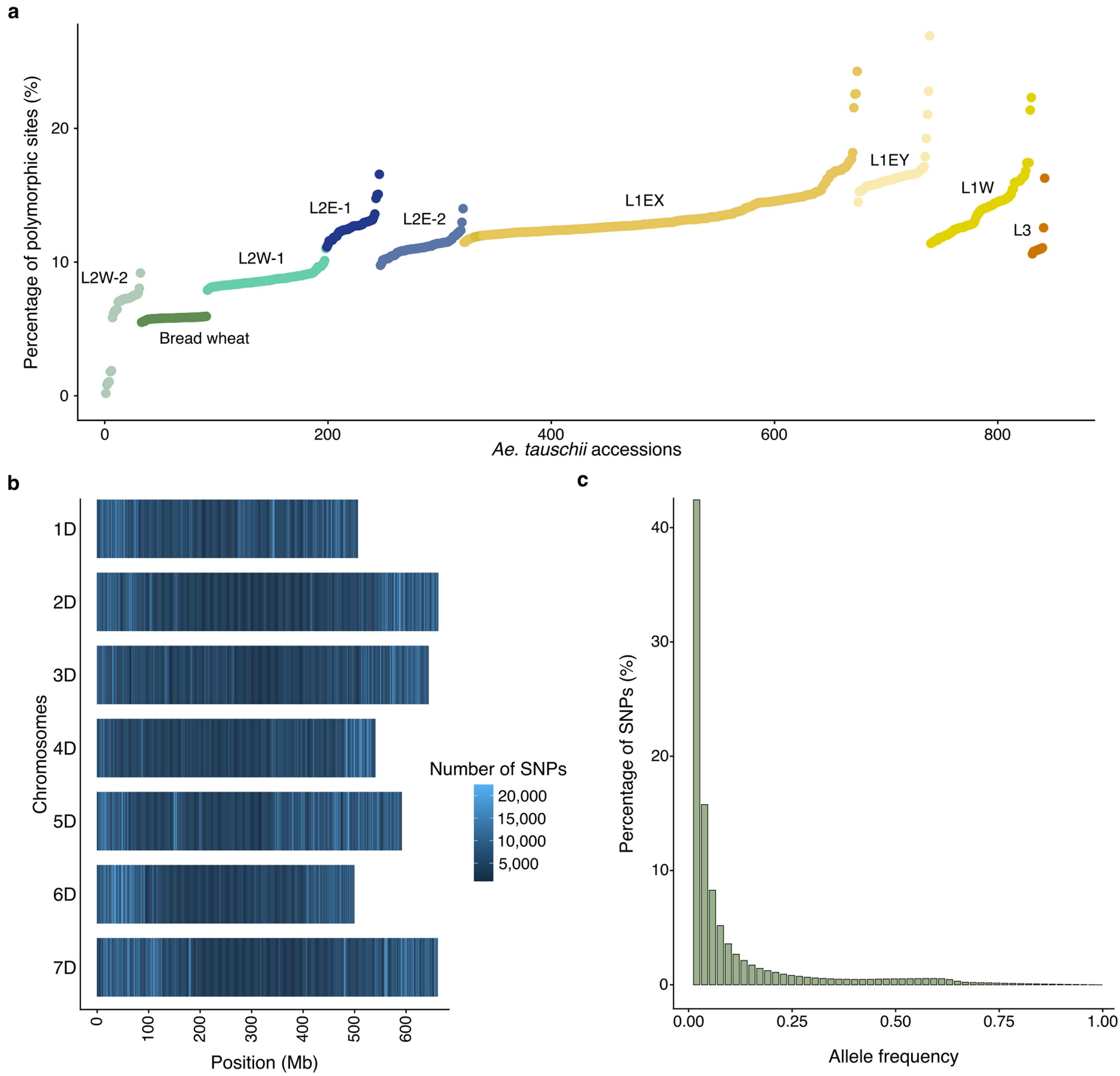

Extended Data Fig. 8 | SNP data statistics. a, The percentage of polymorphic sites for each *Ae. tauschii* accession compared to the TA1675 (L2) reference accession. Each color represents an *Ae. tauschii* or bread wheat group. **b**, SNP density in windows of 1 Mb computed across the 7 chromosomes of TA1675. **c**, Allele frequency distribution.

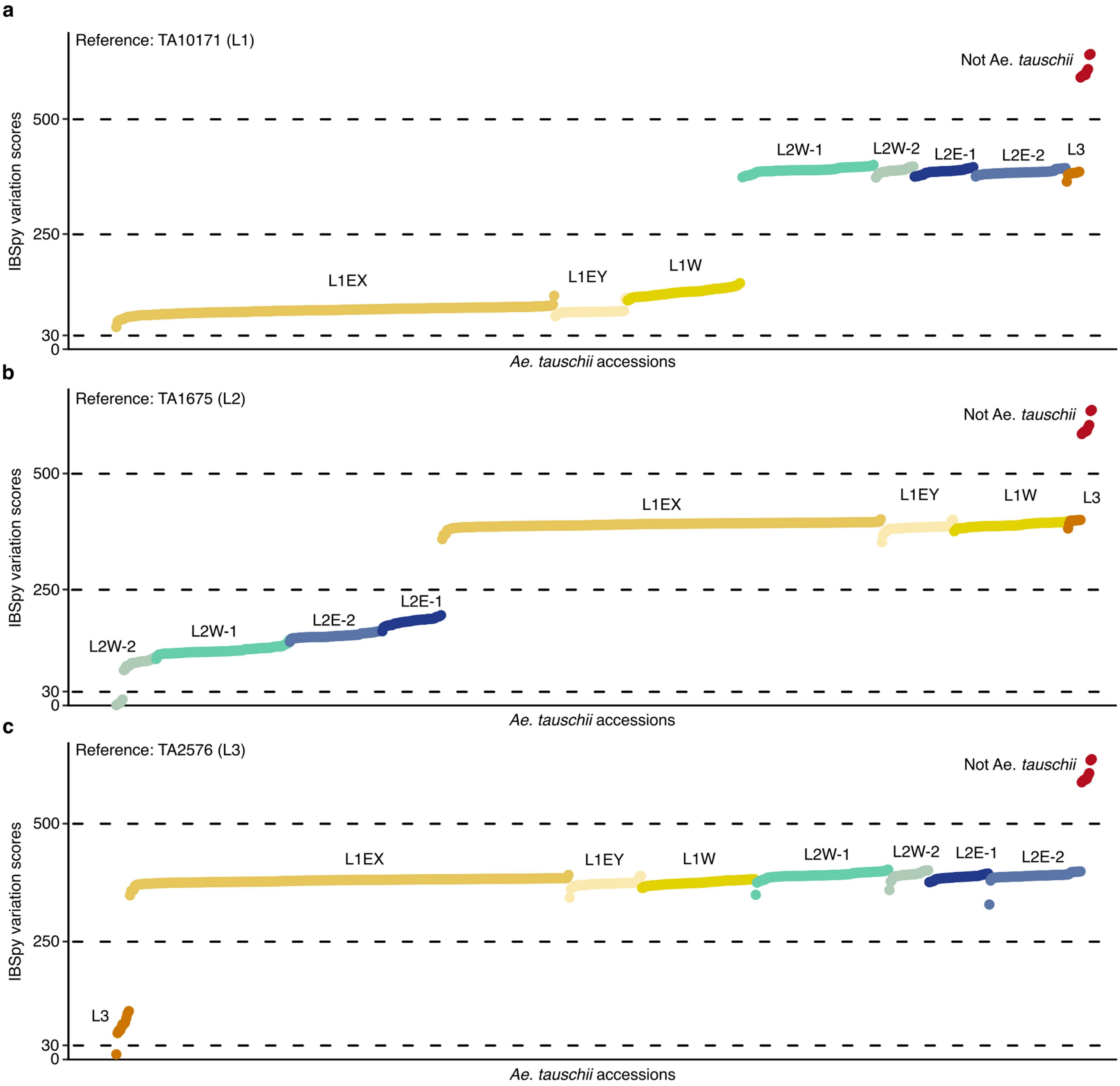

Extended Data Fig. 9 | IBSpy variation score distribution. Shown are the average variation scores for each *Ae. tauschii* accession (represented as a dot) against TA10171 (L1) (**a**), TA1675 (L2) (**b**), and TA2576 (L3) (**c**) (Supplementary Table 32). Based on the distribution, we defined IBSpy values ≤ 30 as identical by state, values > 30 ≤ 250 as being the same *Ae. tauschii* lineage as the reference, values > 250 ≤ 500 as being a different *Ae. tauschii* lineage, and values > 500 as not being *Ae. tauschii*.

Extended Data Table 1 | Assembly statistics for the three chromosome-scale *Aegilops tauschii* references and wheat landrace CWI 86942

Species	*Aegilops tauschii*			*Triticum aestivum*
Accession	**TA10171**	**TA1675**	**TA2576**	**CWI 86942**
Lineage	1	2	3	/
Sequencing coverage (fold)	77	97	67	32
Contig N50 (bp)	53,375,588	221,041,983	116,906,157	44,458,675
Assembly length (bp)	4,151,983,908	4,159,914,615	4,245,074,256	14,571,138,882
Pseudochromosomes	7	7	7	21
Length of pseudochromosomes (bp)	4,106,536,600	4,106,562,375	4,124,033,060	14,470,226,287
Number of unplaced scaffolds	924	884	3,045	3,881
Unplaced scaffold length (bp)	45,447,308	53,352,240	121,041,196	100,912,595
Unplaced scaffold N50 (bp)	49,187	58,980	36,307	82,235
Number of gapped regions	131	32	79	878
Number of HC gene models	44,275	43,511	43,786	147,646*
QV (Phred score)	40.93	48.06	40.3	/
BUSCO score (%)	98.02	98.33	98.14	99.1

*Number of lifted gene models

nature portfolio

Corresponding author(s): Brande B.H. Wulff, Simon G. Krattinger

Last updated by author(s): May 13, 2024

Reporting Summary

Nature Portfolio wishes to improve the reproducibility of the work that we publish. This form provides structure for consistency and transparency in reporting. For further information on Nature Portfolio policies, see our Editorial Policies and the Editorial Policy Checklist.

Statistics

For all statistical analyses, confirm that the following items are present in the figure legend, table legend, main text, or Methods section.

n/a	Confirmed	
□	☒	The exact sample size (*n*) for each experimental group/condition, given as a discrete number and unit of measurement
□	☒	A statement on whether measurements were taken from distinct samples or whether the same sample was measured repeatedly
□	☒	The statistical test(s) used AND whether they are one- or two-sided *Only common tests should be described solely by name; describe more complex techniques in the Methods section.*
☒	□	A description of all covariates tested
☒	□	A description of any assumptions or corrections, such as tests of normality and adjustment for multiple comparisons
□	☒	A full description of the statistical parameters including central tendency (e.g. means) or other basic estimates (e.g. regression coefficient) AND variation (e.g. standard deviation) or associated estimates of uncertainty (e.g. confidence intervals)
□	☒	For null hypothesis testing, the test statistic (e.g. *F*, *t*, *r*) with confidence intervals, effect sizes, degrees of freedom and *P* value noted *Give P values as exact values whenever suitable.*
☒	□	For Bayesian analysis, information on the choice of priors and Markov chain Monte Carlo settings
☒	□	For hierarchical and complex designs, identification of the appropriate level for tests and full reporting of outcomes
☒	□	Estimates of effect sizes (e.g. Cohen's *d*, Pearson's *r*), indicating how they were calculated

Our web collection on statistics for biologists contains articles on many of the points above.

Software and code

Policy information about availability of computer code

Data collection	No software for data collection was used.
Data analysis	The software and tools used in this study are as follows: Core Hunter (v3), hifiasm (v0.16.1), QUAST (v5.0.2), Merqury (v1.3), BUSCO (v5.3.1) with embryophyta_odb10 database for Ae. tauschii and bread wheat accession CWI 86942 primary assemblies, LJA assembler (v0.2), Juicer (v1.6), 3D-DNA (v190716), Juicebox (v2.20.00), RagTag (v2.1.0), MashMap (v3.0.6), QUAST (v5.0.2), BUSCO (v5.3.1), Trimmomatic (v0.38) for Illumina reads, Trimmomatic (v0.40) for RNAseq reads, STAR (v2.7.10b), samtools (v1.8) and (v1.10.0), Braker (v3.0.3), Busco (v5.4.7) with poales_odb10.2019-11-20 database for three Ae. tauschii genome annotations, BLAST+ (v2.9.0-2) and BLAST+(v2.12.0), AGAT (v1.2.1), R (v4.2.0), RStudio (v1db809b8, 2022-05-16) InterProScan (v5.64-96.0), RepeatMasker (v4.1.2-pl) for annotation of Ae. tauschii genomes, InterProScan (v5.55-88.09) for bread wheat accession CWI 86942, liftoff (v1.6.1) and (v1.6.3), gffread (v0.11.7), DIAMOND (v2.1.8), BWA mem (v0.7.17), Bcftools mpileup (v1.9), vcftools (v0.1.16), vcfkit (v0.1.6), pbsv (v2.9.0). Other software utilized to analyse the data are: Python (v3.8), SciPy library (v1.8.0), seaborn Python library (v0.11.2), pbmm2 (v1.10.0), RunAssociation_GLM.py (https://github.com/wheatgenetics/owwc/tree/master/kGWAS), BLAST+ (v2.12.0), MEGA (v11), MapDisto (v2.0), MapChart (v2.32), siFi21-1.2.3-0008, Jellyfish (v 2.3.0), comm bash command, KMC (v3.1.2), IBSpy (v0.4.6), Persephone® Web 0.82 genome browser, QGIS (v3.32.3), OrthoFinder (v2.5.4) R packages used in this study are as follows: ggplot2 (v3.4.2), karyoploteR (v1.20.3), LEA (v3.10.2) package Custom pipelines or scripts generated and used in this study:

Custom script for producing k-mer count matrices for large GWAS panels (https://github.com/githubcbrc/KGWASMatrix)
Custom scripts for missing link finder pipeline and haplotype analysis are available at GitHub (https://github.com/emilecg/wheat_evolution).

For manuscripts utilizing custom algorithms or software that are central to the research but not yet described in published literature, software must be made available to editors and reviewers. We strongly encourage code deposition in a community repository (e.g. GitHub). See the Nature Portfolio guidelines for submitting code & software for further information.

Data

Policy information about availability of data

All manuscripts must include a data availability statement. This statement should provide the following information, where applicable:

- Accession codes, unique identifiers, or web links for publicly available datasets
- A description of any restrictions on data availability
- For clinical datasets or third party data, please ensure that the statement adheres to our policy

The sequencing data and genome assemblies generated in this study were submitted to NCBI under Bioproject number PRJNA956839, including the raw Illumina reads for 350 Aegilops tauschii accessions, the raw PacBio reads, the Hi-C data, the raw RNAseq reads from five tissues of Ae. tauschii accessions TA10171, TA1675 and TA2576, the raw Illumina reads for 59 wheat landraces and the raw PacBio reads and Omni-C data of the wheat landrace CWI 86942.
The genome assemblies of the 46 Ae. tauschii accessions, the assemblies and annotations for CWI 86942, TA10171, TA1675 and TA2576, the variant call (SNP) file, the k-mer matrix for 920 Ae. tauschii accessions, the phylogenetic tree for 493 non-redundant Ae. tauschii accessions, the structural variant call (SV) files, the IBSpy variation tables, the predictions of the subpopulations contributing to the 17 hexaploid wheat assemblies, an excel file containing the RagTag scaffold output agp files and the dot-plots produced by MashMap used to validate the RagTag scaffolding are available at DRYAD (https://doi.org/10.5061/dryad.vmcvdnd0d; https://doi.org/10.5061/dryad.wm37pvmvd; https://doi.org/10.5061/dryad.wpzgmsbvm; https://doi.org/10.5061/dryad.p5hqbzkvx).
The Lr39 genomic sequence was deposited in NCBI Genbank under accession number OR567850.
The TA10171 (L1), TA1675 (L2) and TA2576 (L3) genomes are available for online BLAST, Jbrowse visualisation and synteny analysis with the currently available Triticinae genomes at (https://wheat.pw.usda.gov/GG3pangenome/wheat/D/taus_home.php).
The Ensembl nrTEplants repetitive element database (June 2020) was used for repeat content prediction. Viridiplantae protein models from OrthoDB v.11 were used to predict de novo gene models for the annotated Ae. tauschii genomes. The predicted translated proteins were annotated using the following databases: FunFam, SFLD, PANTHER, Gene3D, PRINTS, Coils, SUPERFAMILY, SMART, CDD, PIRSR, ProSitePatterns, AntiFam, Pfam, MobiDBLite, PIRSF, NCBIfam. We downloaded sequencing data for 306 accessions from NCBI BioProject number PRJNA685125, 275 accessions from NCBI BioProject number PRJNA705859 and 24 accessions from the China National Center for Bioinformation - National Genomics Data Center under accession number PRJCA005979.

Research involving human participants, their data, or biological material

Policy information about studies with human participants or human data. See also policy information about sex, gender (identity/presentation), and sexual orientation and race, ethnicity and racism.

Reporting on sex and gender	No human research participants
Reporting on race, ethnicity, or other socially relevant groupings	N/A
Population characteristics	N/A
Recruitment	N/A
Ethics oversight	N/A

Note that full information on the approval of the study protocol must also be provided in the manuscript.

Field-specific reporting

Please select the one below that is the best fit for your research. If you are not sure, read the appropriate sections before making your selection.

☒ Life sciences □ Behavioural & social sciences □ Ecological, evolutionary & environmental sciences

For a reference copy of the document with all sections, see nature.com/documents/nr-reporting-summary-flat.pdf

Life sciences study design

All studies must disclose on these points even when the disclosure is negative.

Sample size	The 59 bread wheat landraces were sequenced to be representative of the gradient of Lineage 3 introgression dected with the missing link finder pipeline. 46 Ae. tauschii accessions, including representative accessions for each subpopulation and accessions carrying traits of interest, and one bread wheat landrace were selected for genome assemblies. A total of 920 Ae. tauschii accessions were used for the population genomics analyses, sufficient to span the geographical distribution of the species and represent all the different subpopulations with an adequate depth. A total of five different plant tissues per three Ae. tauschii accessions were used to extract RNA for RNA-Seq. A bi-parental mapping population of 123 F2 progenies were generated by crossing leaf rust resistant and susceptible Ae. tauschii accessions. The sizes of the mapping population was based on literature and based on the calculated recombination frequency

Data exclusions

920 out of 955 accessions for which sequencing data was available were included in the population genomic analyses. Accessions were excluded due to low sequencing coverage (less than 5-fold) or duplicate accessions in the different datasets.

Replication

For the RNAseq data, 45 tissue samples were collected: From each of the three accessions, three biological replicates were taken from each of: young leaf, root, stem, flag leaf and inflorescence; all replicates were successful and none were discarded for the analysis. For VIGS, five biological replicates were used to test each silencing probe and the experiment was repeated three times, showing every time the same result. For rust phenotyping Ae. tauschii bi-parental mapping population, at least 15 seedlings of F2:3 families were screened to access the homozygous resistant, homozygous susceptible and segregating lines.

Randomization

Viral and rust inoculated plants were allocated randomly among groups.

Blinding

Blinding was performed when rust phenotyping plants (i.e., the genotype of the plant was not known when phenotyping the mapping populations)

Reporting for specific materials, systems and methods

We require information from authors about some types of materials, experimental systems and methods used in many studies. Here, indicate whether each material, system or method listed is relevant to your study. If you are not sure if a list item applies to your research, read the appropriate section before selecting a response.

Materials & experimental systems

n/a	Involved in the study	
☒	☐	Antibodies
☒	☐	Eukaryotic cell lines
☒	☐	Palaeontology and archaeology
☒	☐	Animals and other organisms
☒	☐	Clinical data
☒	☐	Dual use research of concern
☐	☒	Plants

Methods

n/a	Involved in the study	
☒	☐	ChIP-seq
☒	☐	Flow cytometry
☒	☐	MRI-based neuroimaging

Plants

Seed stocks

Seed of 228 non-redundant accessions were obtained from the Open Wild Wheat Consortium Ae. tauschii Diversity Panel collection deposited at the Germplasm Resource Unit (GRU) of the John Innes Centre; 48 accessions from the Cereal Crop Wild Relatives (Triticeae) collection of the GRU; 19 accessions from the DFW Wheat Academic Toolkit collection of the GRU that have been used as synthetic hexaploid wheat D-genome donors; 223 accessions from the Wheat Genetics Resource Center (WGRC) of Kansas State University; 34 accessions from the Plant Gene Resources of Canada (PGRC); 84 accessions collected from Tajikistan and donated by the Institute of Botany, Plant Physiology and Genetics of the Tajikistan National Academy of Sciences; 20 accessions donated by the Azerbaijan National Academy of Sciences; and 37 accessions collected from Pakistan and donated by Quaid-i-Azam University. Accession P-99.95-1.1 was obtained from the Deposited Published Research Material collection of the GRU. 57 bread wheat landraces were received from International Maize and Wheat Improvement Center (CIMMYT) and three bread wheat landraces were obtained from the International Center for Agricultural Research in the Dry Areas (ICARDA).

Novel plant genotypes

N/A

Authentication

N/A